

1 Identification of a long non-coding RNA regulator of liver carcinoma 2 cell survival 3

4 *Yulia Rybakova*^{1,2}, *John T. Gonzalez*¹, *Roman Bogorad*¹, *Vikash P. Chauhan*¹, *Yize L. Dong*^{3,4},
5 *Charles A. Whittaker*¹, *Victor Koteliansky*², and *Daniel G. Anderson*^{1,5,6,7,8*}
6

- 7 1) David H. Koch Institute for Integrative Cancer Research, Massachusetts Institute of
8 Technology, Cambridge, MA 02142, USA
- 9 2) Skolkovo Institute of Science and Technology, Moscow, 121205, Russia
- 10 3) Department of Electrical Engineering and Computer Science, Massachusetts Institute of
11 Technology, Cambridge, MA 02142, USA
- 12 4) Department of Biology, Massachusetts Institute of Technology, Cambridge, MA 02142,
13 USA
- 14 5) Institute for Medical Engineering and Science, Massachusetts Institute of Technology,
15 Cambridge, MA 02139, USA
- 16 6) Harvard and MIT Division of Health Science and Technology, Massachusetts Institute of
17 Technology Cambridge, MA 02139, USA
- 18 7) Department of Chemical Engineering, Massachusetts Institute of Technology, Cambridge
19 MA 02139, USA

20
21 * Correspondence: dgander@mit.edu
22

23 **KEYWORDS:** lncRNA, liver cancer, RNAi, LNA, CRISPR/Cas9, functional genetic screen, cancer
24 cell survival
25

26 **ABSTRACT**

27 Genomic studies have significantly improved our understanding of hepatocellular carcinoma
28 (HCC) biology and have led to the discovery of multiple protein-coding genes driving
29 hepatocarcinogenesis. In addition, these studies have identified thousands of new non-coding
30 transcripts deregulated in HCC. We hypothesize that some of these transcripts may be involved
31 in disease progression. Long non-coding RNAs are a large class of non-coding transcripts which
32 participate in the regulation of virtually all cellular functions. However, a majority of lncRNAs
33 remain dramatically understudied. Here, we applied a pooled shRNA-based screen to identify
34 lncRNAs essential for HCC cell survival. We validated our screening results using RNAi,
35 CRISPRi, and antisense oligonucleotides. We found a lncRNA, termed ASTILCS, that is critical
36 for HCC cell growth and is overexpressed in tumors from HCC patients. We demonstrated that
37 HCC cell death upon ASTILCS knockdown is associated with apoptosis induction and
38 downregulation of a neighboring gene, Protein Tyrosine Kinase 2 (PTK2), a crucial protein for
39 HCC cell survival. Taken together, our study describes a new, non-coding RNA regulator of HCC.
40
41
42
43
44
45
46
47
48
49
50

51 INTRODUCTION

52 Liver cancer is one of the leading causes of cancer mortality worldwide, accounting for
53 more than 700,000 deaths per year [1]–[3]. Hepatocellular carcinoma (HCC) is the most frequent
54 subtype of liver cancer. Despite recent progress in HCC treatment it remains one of the deadliest
55 types of cancer [3], [4]. Notably, the incidence of HCC has been increasing in recent decades,
56 making HCC one of the fastest-growing causes of death worldwide [5], [6]. This poor prognosis
57 underlines the need for new effective therapies. Better understanding of the molecular
58 mechanisms regulating HCC progression may yield new potential drug targets.

59 A meta-analysis of human HCC datasets revealed 935 genes for which expression was
60 significantly dysregulated in HCC samples compared to healthy tissues [7]. Further Gene
61 Ontology analysis of these genes identified several gene networks associated with HCC
62 progression. Among them were upregulation of cell proliferation, downregulation of apoptosis,
63 loss of hepatocyte differentiation, immunosuppression, and activation of proteins acting at an
64 epigenetic level [7]. Comprehensive genomic profiling of patient HCC samples and their
65 comparison with healthy tissues have helped uncover molecular changes promoting the above
66 phenotypic features of HCC [8]–[15]. Among them, mutations leading to activation of the WNT
67 signaling pathway were most common [9]–[14], [16], implicating the WNT pathway as a major
68 driver of hepatocarcinogenesis [17], [18]. Moreover, activation of the WNT pathway is associated
69 with an immunosuppressive microenvironment, another hallmark of HCC progression [8], [15],
70 which emphasizes the role of WNT pathway activity in HCC progression. Other common
71 mutations affected the TERT promoter, TP53, genes regulating cell cycle, PI3K-AKT-mTOR
72 signaling and cell differentiation [9]–[14]. Notably, up to 50% of clinical HCC samples reported in
73 different studies have a mutation in chromatin modifiers [9]–[13], indicating the importance of
74 epigenetic regulation in HCC development.

75 Besides shedding light on the roles of protein-coding genes, integrative genomic studies
76 have revealed that the majority (>70%) of transcribed sequences in the human genome
77 participate in cell function regulation without producing a protein [19], [20]. Long non-coding RNAs
78 (lncRNAs) are defined as non-coding transcripts longer than 200 nucleotides and represent a
79 large class of non-coding elements, comprising more than 50,000 annotated transcripts to date
80 [21]–[25]. Pertinently, hundreds of lncRNAs are recurrently deregulated in HCC, suggesting
81 potential roles in hepatocarcinogenesis. Co-expression network analysis determined that these
82 lncRNAs were associated with cell proliferation, metastasis, immune response, and liver
83 metabolism – hallmarks of HCC progression [26]–[29]. While the pathogenic roles of some of
84 these lncRNAs (e.g. HULC, H19, HOTAIR, HOTTIP, DANCR) have already been described [30]–
85 [32], a plurality of lncRNA transcripts remain largely uncharacterized. Discovery of novel lncRNAs
86 and their intracellular functions promises to expand our knowledge of HCC cellular physiology
87 and may provide the basis for new therapeutic modalities.

88 Currently, lncRNA functions cannot easily be predicted based on their sequence. Instead,
89 subcellular localization, transcript abundance, and functional genomic screens can help to
90 efficiently narrow down possible lncRNA biological roles and molecular functions [33]–[37]. For
91 instance, lncRNAs located mainly in the nucleus typically function as transcription regulators of
92 local genes (*in cis*) or distant genes (*in trans*) [36]. Cytoplasmic lncRNAs are more likely to
93 regulate protein production, formation of post-translational modifications, and sequestration of
94 miRNAs or RNA-binding proteins [37]. Transcript abundance can provide another hint about
95 lncRNA function. For example, low-abundance transcripts tend to function *in cis* because their
96 low concentration makes diffusion a barrier to activity at long distances from the transcription site.
97 Abundant lncRNAs, on the other hand, can achieve high concentrations at multiple target regions,
98 including those outside of the nucleus and therefore often function *in trans* [33]. Finally, pooled
99 functional genetic screens are a powerful tool allowing for parallel perturbation of multiple genes
100 to select for those that are critical for a phenotype or function [38]–[40]. Recently, genome-wide
101 screens have made it possible to identify lncRNAs involved in a wide variety of cellular functions

102 including cell proliferation, drug resistance, autophagy, tissue homeostasis, and cell differentiation
103 [41]–[46].

104 RNA interference (RNAi) is an effective method for transient silencing of gene expression
105 and therefore is an instrument for loss-of-function genetic screens [38], [40]. Previously, it was
106 reported that RNAi-mediated gene silencing is restricted to the cytoplasm, limiting targeting of
107 nuclear transcripts. However, recent studies suggest RNAi presence and activity in the
108 mammalian nucleus as well, although with less efficiency [47]–[50]. Clustered regularly
109 interspaced short palindromic repeat interference (CRISPRi) is another potent technique for
110 lncRNA silencing [39], [51], [52]. However, using CRISPRi to regulate a lncRNA overlapping with
111 other transcripts might contribute to the expression of that transcript, confounding data
112 interpretation [53]. Given promoters of most lncRNAs are poorly annotated and lncRNAs often
113 overlap with protein-coding genes (or their promoters/enhancers), in our screen, we chose to
114 perturb lncRNA at the RNA level. We performed an shRNA-based pooled screen to identify
115 lncRNAs essential for the survival of the human HCC cell line HUH7. Based on the lncRNA
116 expression profile of these cells, we designed a lentiviral shRNA library targeting all identified
117 lncRNAs. Using this library, we performed a loss-of-function genetic screen and found that
118 lncRNA ENST00000501440.1 is critical for HUH7 cell growth. We named this lncRNA ASTILCS
119 (**AntiSense Transcript Important for Liver Carcinoma Survival**). Importantly, in patient data,
120 ASTILCS is significantly overexpressed in HCC compared to normal tissues. Further, using gene
121 manipulation techniques, we demonstrate that ASTILCS knockdown results in apoptosis
122 induction and HCC cell death. Finally, we show that ASTILCS knockdown correlates with
123 downregulation of a neighboring gene expressing Protein Tyrosine Kinase 2 (PTK2), the silencing
124 of which results in HCC cell death.

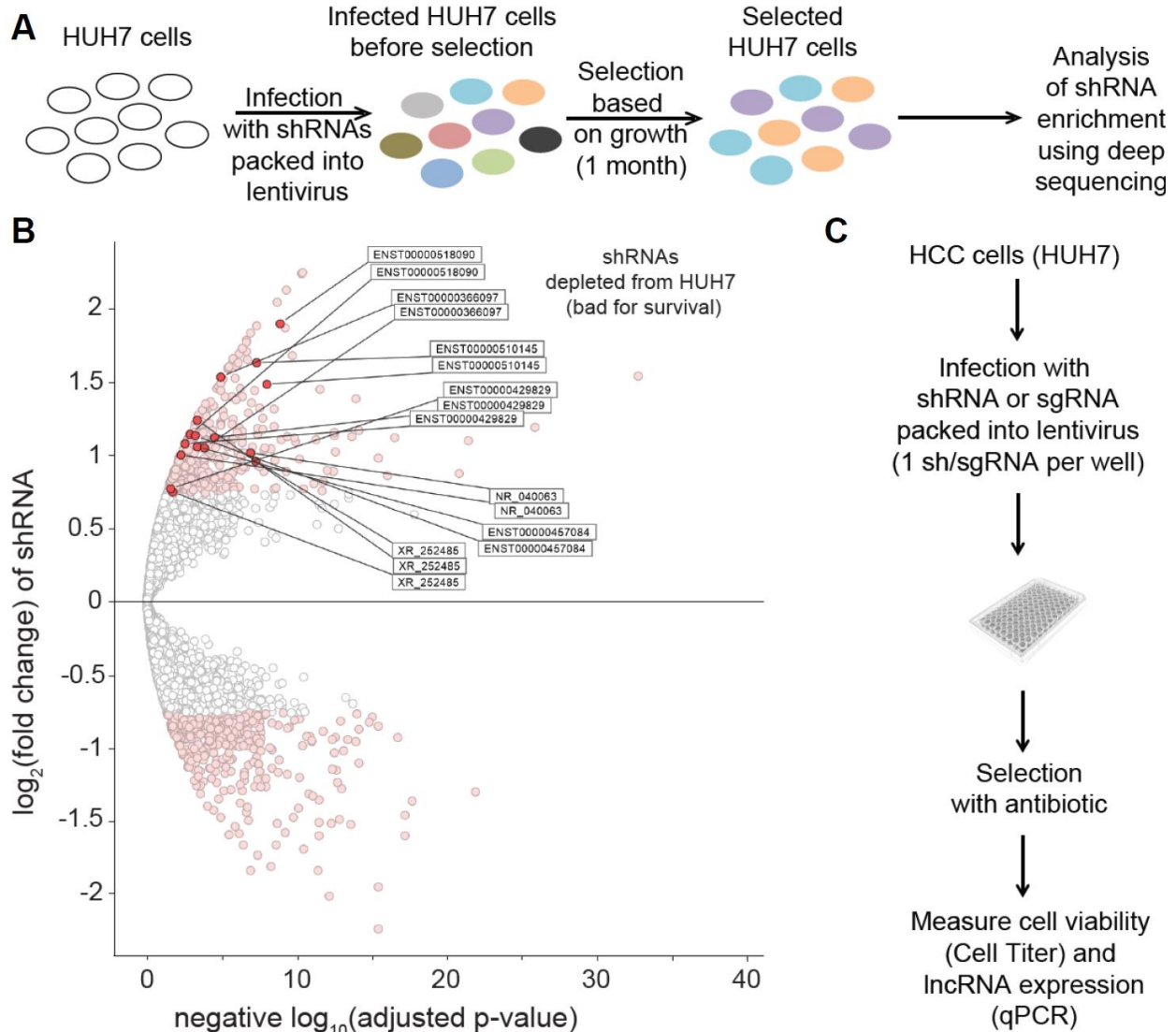
125 126 **RESULTS**

127 128 **Pooled RNAi-based screen identifies lncRNAs potentially essential for HCC cell** 129 **survival**

130 To design the shRNA library, we performed transcriptome analysis in HUH7 HCC cell line
131 and identified 1618 non-coding RNA transcripts longer than 200 base pairs and expressed at a
132 level higher than 5 FPKM (Supplemental Fig. 1, Supplemental Table 1). Next, we constructed a
133 library of 7873 shRNA vectors to knockdown the identified lncRNAs based on RNAi and applied
134 on HUH7 cells (Fig. 1A). Each lncRNA was targeted by 4-5 shRNAs to account for shRNA off-
135 target effects. To identify lncRNAs important for HUH7 cell survival, shRNAs present in the final
136 population were compared to shRNA representation in the input library. A lncRNAs was
137 considered a candidate when at least two of its corresponding shRNAs were underrepresented
138 in the final population with $\log_2(\text{fold change compared to control}) \geq 1$ or by at least 3 shRNAs with
139 $\log_2(\text{fold change compared to control}) \geq 0.75$ (Fig. 1B). With these constraints, we identified seven
140 lncRNA candidates for further validation (ENST00000429829, ENST00000510145,
141 ENST00000457084, ENST00000501440.1, ENST00000366097.2, ENST00000518090 and
142 ENST00000421703.5). To the best of our knowledge only ENST00000429829 and
143 ENST00000510145 very previously characterized [54]–[60].

144 Both of these lncRNAs have been identified in the context of cancer. Although their
145 mechanisms are the focus of active discussion, their presence among our screen hits supports
146 the likelihood that the rest of the transcripts are also involved in HCC survival and biology.
147 ENST00000429829 is one of the multiple transcripts of gene ENSG00000229807, also known as
148 XIST. In addition to its established role as the master regulator of X chromosome inactivation [61],
149 XIST has been reported to participate in progression of a variety of cancers, including HCC [54]–
150 [58], [62]–[64]. However, the results of these studies are controversial [54]–[58].
151 ENST00000510145 is one of nine transcripts of gene ENSG00000250682, also known as
152 LINC00491 or BC008363. This gene was found to be upregulated in a TCGA colon

153 adenocarcinoma dataset and was associated with lower patient survival, implying
 154 ENSG00000250682 importance for colorectal cancer progression [59]. Conversely, in pancreatic
 155 ductal adenocarcinoma patients LINC00491 expression was significantly lower compared to the
 156 control group and was associated with better survival rates [60].
 157



158
 159 **Figure 1. Experimental design and selection strategy for the identification of lncRNAs**
 160 **essential for HUH7 HCC cell survival.** **A.** Schematic workflow of the survival-based pooled
 161 shRNA library screen in HUH7 cells. shRNAs were designed to target lncRNAs identified in the
 162 cell line. **B.** Volcano plot of the differentially expressed shRNAs in the final population of HUH7
 163 cells. The x-axis indicates the adjusted p values plotted in $-\log_{10}$. The y-axis indicates the
 164 $\log_2(\text{fold change})$ in gene expression, which was defined as the ratio of normalized gene
 165 expression in the input library over the final HUH7 population. Light red dots represent shRNAs
 166 with $\log_2\text{FC} \geq 0.75$ and adjusted $p\text{-value} \leq 0.05$. Dark red dots represent shRNAs of lncRNAs for
 167 which at least 2 shRNAs have $\log_2\text{FC} \geq 1$ and adjusted $p\text{-value} \leq 0.05$ or lncRNAs for which at least
 168 3 shRNAs have $\log_2\text{FC} \geq 0.75$ and adj $p\text{-va} \leq 0.05$. **C.** Schematic workflow of arrayed shRNA and
 169 sgRNA screens used for validation of lncRNAs identified in B.

170
 171

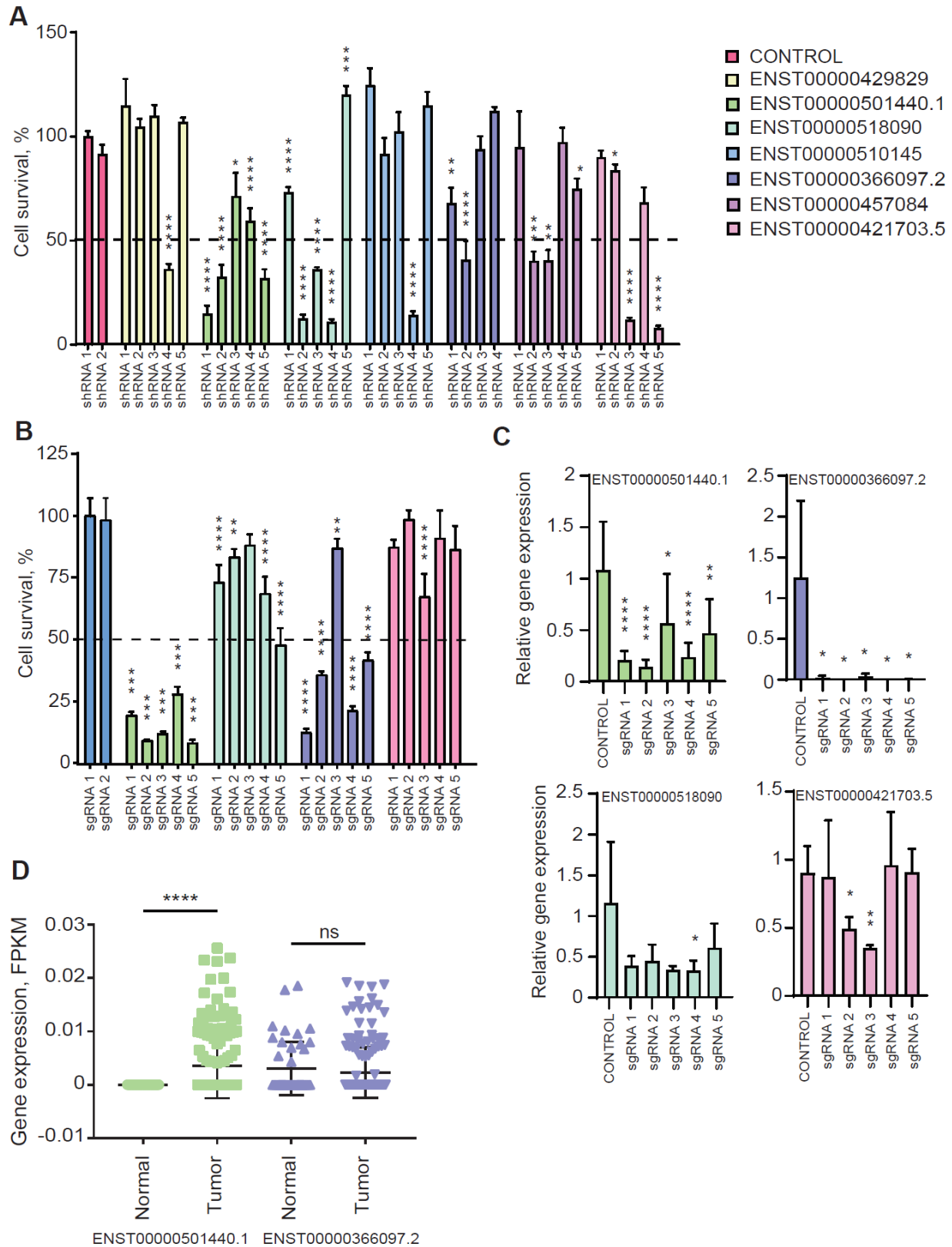
172 **Validation of the screen results identifies lncRNA ASTILCS as a new regulator of**
173 **HCC cell survival**

174 To validate the screening results, we individually expressed the five library shRNAs for
175 each of the seven candidate lncRNAs (Supplemental Table 2) and repeated the screen in an
176 arrayed format (Fig. 1C). Those lncRNAs for which at least two corresponding shRNAs reduced
177 cell survival by more than 50% compared to the control shRNAs were selected for further analysis;
178 these were ENST00000501440.1, ENST00000366097.2, ENST00000518090, and
179 ENST00000421703.5 (Fig. 2A).

180 RNAi-based gene silencing is associated with a few pitfalls, particularly off-target activity
181 and variability in knockdown efficiency [65], [66]. We therefore further validated the candidate
182 lncRNAs using an arrayed screen based on CRISPRi (Fig. 1C). To do so, we designed five
183 sgRNAs (Supplemental Table 3) to allow targeting of each candidate lncRNA by CRISPRi (Fig.
184 2B, C). Among the four studied lncRNAs, CRISPRi-mediated knockdown of only
185 ENST00000501440.1 and ENST00000366097.2 resulted in substantially decreased survival for
186 HUH7 HCC cells (Fig. 2B, C). Specifically, 5/5 sgRNAs targeting lncRNA ENST00000501440.1
187 decreased HCC cell survival by more than 70% and 4/5 sgRNAs targeting lncRNA
188 ENST00000366097.2 resulted in more than 50% HUH7 cell death. In contrast, knockdown of
189 ENST00000518090 was not associated with a notable decrease in HCC cell survival and only 2/5
190 sgRNAs designed to target ENST00000421703.5 induced partial lncRNA knockdown with mild
191 effects on HCC cell survival. Based on these results we concluded that ENST00000501440.1 and
192 ENST00000366097.2 expression is critical for HCC cell survival. ENST00000501440.1 is the only
193 transcript of ENSG00000244998 gene. It is a 1380 bp long antisense transcript comprised of 2
194 exons. ENST00000366097.2 is one of two transcripts of ENSG00000203266 gene. It is a 770 bp
195 long intergenic lncRNA consisting of 3 exons. Both transcripts are predicted to have low coding
196 potential and are not conserved in chimpanzee or mouse [67]. Thus, we identified two novel
197 lncRNA genes which expression is potentially important for HCC cell survival.

198 To determine whether these two lncRNAs are HCC specific or are present in healthy liver
199 tissues, we examined ENST00000501440.1 and ENST00000366097.2 expression in tissue
200 samples from patients with HCC using a dataset from The Cancer Genome Atlas (TCGA-LIHC-
201 rnaexp, downloaded from The Atlas of lncRNA in Cancer (TANRIC) [68]). We found that
202 ENST00000501440.1 expression was significantly higher in liver cancer samples compared to
203 the adjacent tissue (Fig. 2D; $p < 0.0001$). Yet, lncRNA expression was not associated with patient
204 survival [68]. These data suggest that only ENST00000501440.1 expression is critical for the
205 survival of tumor cells. Because only ENST00000501440.1 expression is differentially expressed
206 in cancer cells, we selected it for further analysis. Through the rest of the publication, we refer to
207 this lncRNA by the name of ASTILCS (**AntiSense Transcript Important for Liver Carcinoma**
208 **Survival**).

209



210
211
212

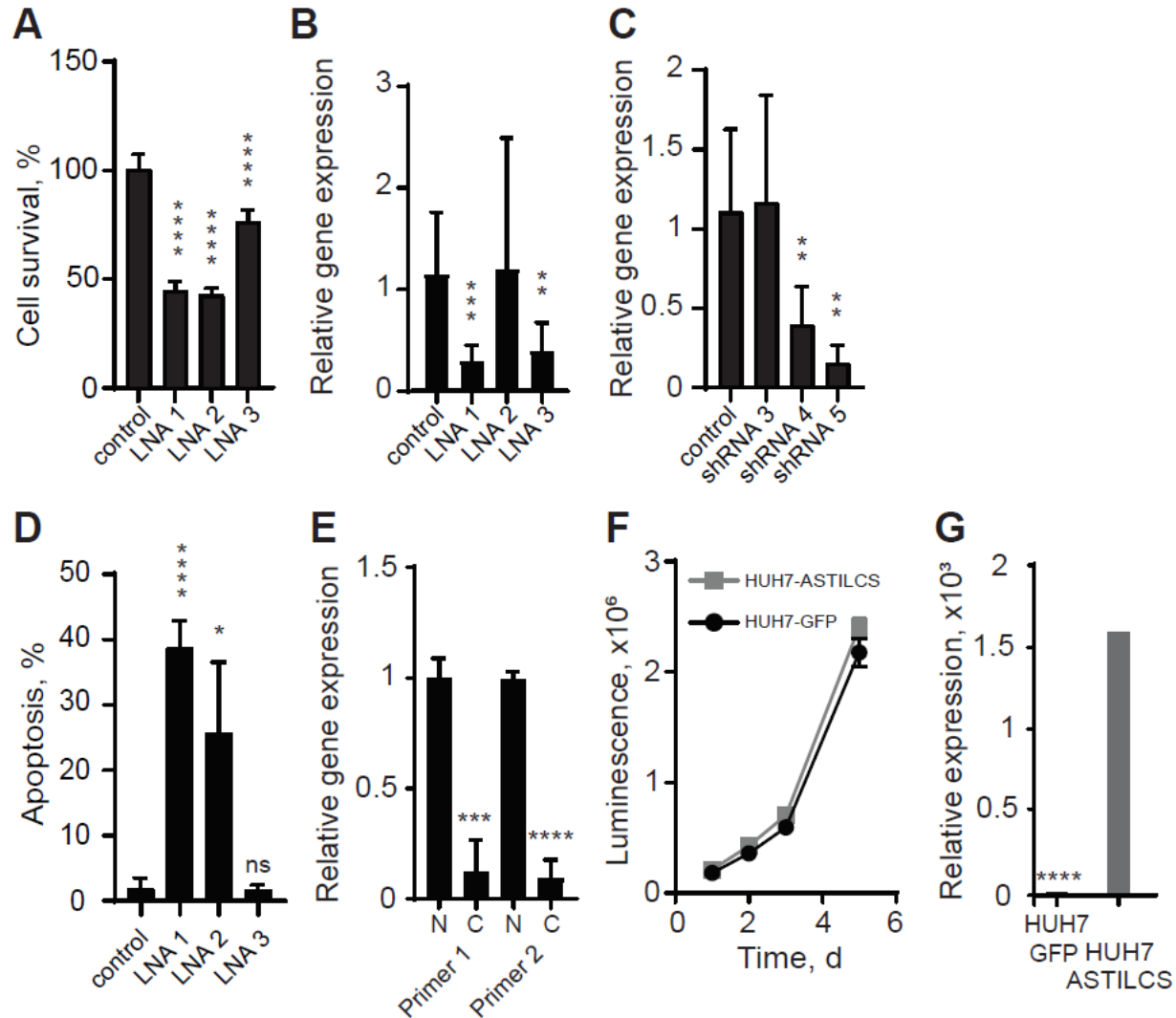
Figure 2. Validation of the screen results identifies lncRNA ASTILCS a new regulator of HCC cell survival. A. HUH7 cell survival upon shRNA-mediated knockdown of candidate

213 *lncRNAs (compared to shRNA1), n≥3. B. HUH7 cell survival upon CRISPRi-mediated knockdown*
214 *of candidate lncRNAs from A. Compared to control sgRNA1, n≥3. C. LncRNA expression in HUH7*
215 *cells transduced with sgRNA-dCas9-KRAB targeting one of the candidate lncRNAs, n≥4. D.*
216 *ENST00000501440.1 (ASTILCS) and ENST00000366097.2 expression in HCC vs adjacent*
217 *tissue (TCGA-LIHC-rnaexp dataset#), n≥45. All values are mean ± SD, **** p < 0.0001; *** p <*
218 *0.001; ** p < 0.01; * p < 0.05.*
219

220 A closer look into the ASTILCS locus revealed that ASTILCS is an antisense sequence to
221 the protein-coding gene Protein Tyrosine Phosphatase Type IVA 3 (PTP4A3) (Supplemental Fig.
222 2). PTP4A3 is known to be important for cell proliferation; its knockdown has been shown to
223 decrease survival in multiple types of cells [69]–[73]. Because sgRNAs targeting ASTILCS bind
224 PTP4A3 between 512 and 611 bp away from the transcription start site, there is a possibility that
225 the sgRNA-dCas9-KRAB complex hinders PTP4A3 expression, resulting in HCC cell death
226 independently of ASTILCS. Indeed, expression analysis of the sgRNA treated cells revealed deep
227 knockdown of PTP4A3 (Supplemental Fig. 3). To add orthogonal evidence of ASTILCS
228 prosurvival effects on HCC cells, we knocked down its expression by transient transfection of
229 antisense oligonucleotides containing locked nucleic acid modifications (LNA) (Supplemental
230 Table 4). LNAs bind with high affinity to complementary RNA sequences forming DNA•RNA
231 hybrids, which are recognized and cleaved by RNase H1, resulting in gene knockdown [74]–[76].
232 We observed a reduction in HUH7 HCC cell survival upon treatment with the LNAs (Fig. 3A),
233 which was associated with ASTILCS knockdown (Fig. 3B). We noticed that, despite a decrease
234 in cell survival in LNA2-treated samples, ASTILCS RNA levels in these samples were not affected.
235 These findings may be explained by previous reports demonstrating that antisense
236 oligonucleotide hybridization with RNA can affect its function without inducing degradation [77],
237 [78]. Thus, LNA2 binding to ASTILCS might perturb its function via steric blocking of lncRNA
238 secondary structure formation or interaction with molecules important for the lncRNA signaling
239 [79]–[81]. To further corroborate whether ASTILCS expression is critical for HCC cell survival, we
240 measured its expression in HUH7 HCC cells transfected with the 3 most efficient shRNAs from
241 the library (Supplemental Fig. 4) and observed dosage-dependent decrease in HCC cell survival
242 (Fig. 3C and Fig. 2A). These findings substantiate that ASTILCS regulates HCC cell survival and
243 its specific knockdown leads to HCC cell death independently of its reciprocal sense coding gene,
244 PTP4A3.
245

246 **LncRNA ASTILCS knockdown in HCC cells results in apoptosis induction**

247 To understand the molecular mechanism of the effects of ASTILCS on HCC cell survival,
248 we studied whether ASTILCS knockdown affects HUH7 HCC cell apoptosis. To that end, we
249 performed a TUNEL assay to assess apoptosis. We found that transfection with shRNA
250 expressing plasmids or treatment with LNAs led to a dose-dependent increase in the number of
251 apoptotic cells (Fig. 3D and Supplemental Figure 5). Differences in the apoptotic cell number
252 between shRNA and LNA treated samples were likely due to experimental constraints in the
253 knockdown techniques. Apoptosis levels in LNA-treated samples were measured 24 h after the
254 treatment, while in shRNA-treated samples apoptosis could only be measured 4 days after
255 transduction, providing time for compensation mechanisms to occur. Moreover, cell media in
256 shRNA-treated samples had to be changed to remove the lentiviral particles and add selective
257 agent, which could also result in partial removal of poorly attached apoptotic cells. From our
258 findings we conclude that ASTILCS knockdown results in the induction of apoptosis and a
259 subsequent decrease in HUH7 cell survival.
260



261
 262 **Figure 3. ASTILCS expression is essential for liver carcinoma cell survival.** **A.** HUH7 cell
 263 survival 48h after transfection with LNAs targeting ASTILCS, $n \geq 6$. **B.** ASTILCS expression in
 264 HUH7 cells transfected with LNAs targeting ASTILCS, $n \geq 5$. **C.** ASTILCS expression in HUH7 cells
 265 transduced with shRNAs targeting ASTILCS, $n \geq 5$. **D.** Apoptosis in HUH7 cells treated with LNAs
 266 targeting ASTILCS, $n = 3$. **E.** LncRNA expression in nucleus and cytoplasm, $n \geq 8$. **F.** Growth curve
 267 for HUH7 cells transfected with GFP and ASTILCS. **G.** ASTILCS expression in HUH7 cells
 268 transduced with ASTILCS-TRC209, $n = 3$. All values are mean \pm SD, **** - $p < 0.0001$; *** - $p <$
 269 0.001 ; ** - $p < 0.01$; * - $p < 0.05$; ns. - $P > 0.05$.

270

271 **ASTILCS is a nuclear antisense transcript which functions in cis**

272 As subcellular localization can hint towards the molecular mechanism of a lncRNA, we
 273 measured ASTILCS transcript levels in nuclear and cytoplasmic extracts and found ASTILCS
 274 RNA to be strongly enriched in the nucleus (Fig. 3E). These results are in line with the relatively
 275 low expression level of ASTILCS in HUH7 cells (~ 23.5 FPKM, Supplemental Figure 5), a common
 276 feature of nuclear transcripts. Further, to classify the mechanism by which ASTILCS knockdown
 277 decreases HCC cell survival, we determined whether ASTILCS functions in *cis* or *trans*. To do
 278 so, we overexpressed cDNA encoding ASTILCS from a randomly integrated lentivirus and
 279 assessed cell proliferation as the population doubling time (Td). We found that the Td of cells
 280 overexpressing ASTILCS (1.13 ± 0.07 days) was similar to the Td of control cells expressing green

281 fluorescent protein (GFP) from the same vector (1.13 ± 0.03 days, $p=0.17$) (Fig. 3F, G and
282 Supplemental Table 5). Because we did not observe any gain in survival for cells overexpressing
283 ASTILCS, we concluded that ASTILCS is not likely to act in *trans* and that its effects on HCC cell
284 survival are probably associated with *cis* functions.

285

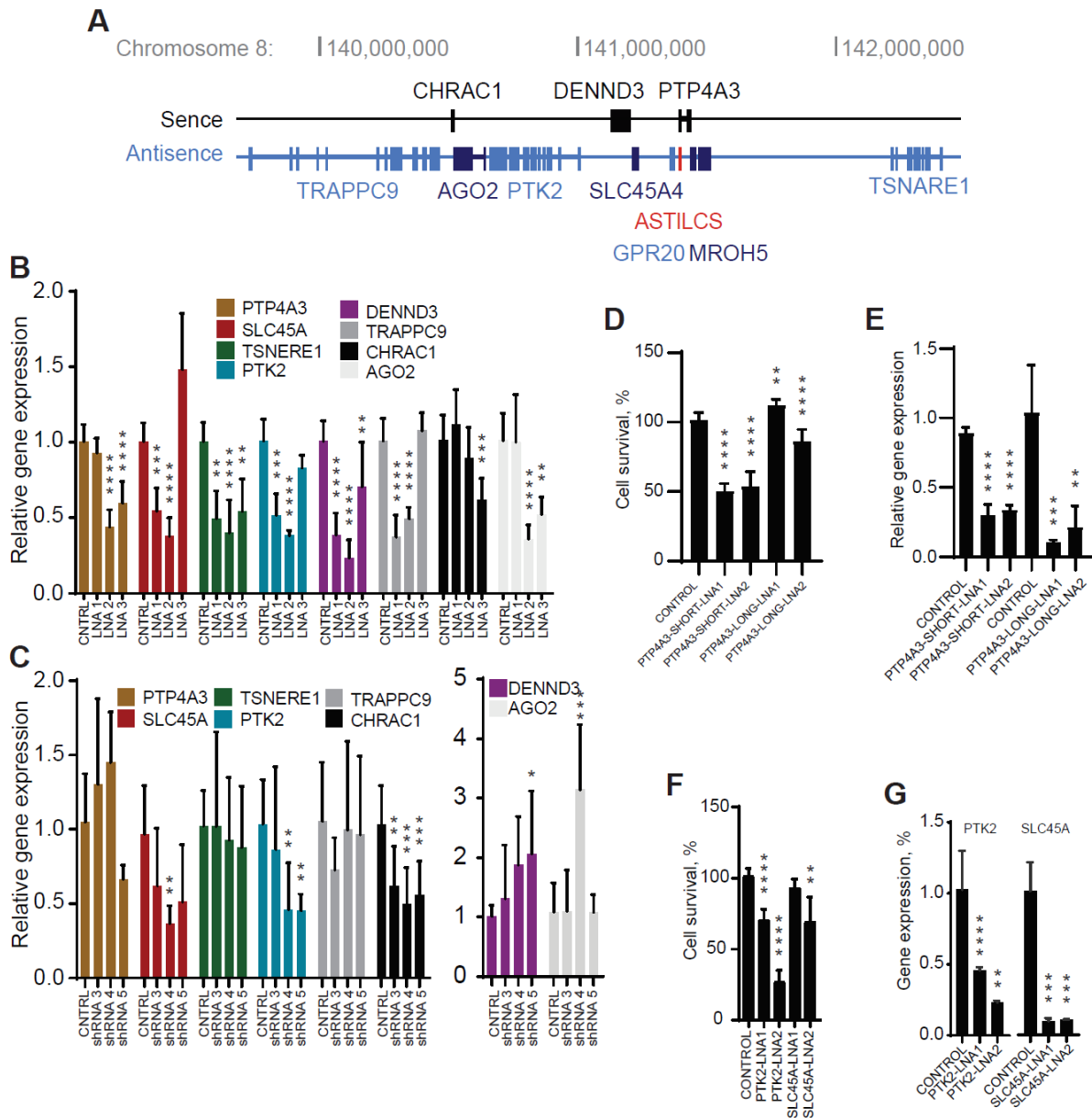
286 **ASTILCS silencing is associated with downregulation of neighboring gene PTK2** 287 **essential for HCC cell survival**

288 The effects of low abundance nuclear cis-acting lncRNAs occur typically in the loci from
289 which they are transcribed. Those effects can be mediated by: 1) the lncRNA transcripts
290 themselves; 2) the act of lncRNA transcription; or 3) the regulatory DNA elements within the
291 lncRNA locus [82], [83]. To determine whether the investigated phenotype might result from
292 ASTILCS transcript effects on local gene expression, we examined the impact of ASTILCS
293 knockdown on the expression of all genes within 1 Mb of the target site (Fig. 4A). Analysis of the
294 HUH7 HCC cell transcriptome revealed that G Protein-Coupled Receptor 20 (GPR20) and
295 Maestro Heat Like Repeat Family Member 5 (MROH5) are not expressed in HUH7 cells
296 (Supplemental Table 6), so they were removed from consideration. We found that LNA-induced
297 ASTILCS knockdown led to a change in expression of all studied genes in the locus (Fig. 4B).
298 Only downregulation of Solute Carrier Family 45 Member 4 (SLC45A4), Protein Tyrosine Kinase
299 2 (PTK2), DENN Domain Containing 3 (DENND3) and Trafficking Protein Particle Complex 9
300 (TRAPPC9) led to a dose-dependent decrease in both ASTILCS expression and HCC cell survival
301 (Fig. 4B, see also Fig. 3A and B). In contrast, shRNA-mediated knockdown of ASTILCS was
302 associated with downregulation of SLC45A, PTK2, and Chromatin accessibility complex protein
303 1 (CHRAC1) (Fig. 4C, see also Fig. 2A and 3C). Genes that were inconsistent across ASTILCS
304 knockdown approaches were considered to be results of indirect or off-target effects. Because
305 only SLC45A and PTK2 expression was affected in the same manner by both shRNAs and LNAs,
306 we inferred that ASTILCS knockdown potentially induces HCC cell death via downregulation of
307 one or both of these genes. Changes in expression of other genes might be a result of indirect
308 effects of ASTILCS downregulation or simply off-target effects of the LNAs and shRNAs.

309 LncRNAs located antisense to protein coding genes are often found to regulate activity of
310 their sense pair in different manners [84], [85]. Surprisingly, even though protein-coding gene
311 PTP4A3 is located antisense to ASTILCS, we did not observe an apparent effect of ASTILCS
312 knockdown on PTP4A3 expression (Fig. 4B, C). This indicates that the ASTILCS transcript itself
313 does not affect the expression of PTP4A3. Next, we studied whether PTP4A3 knockdown can
314 affect HUH7 HCC cell survival. PTP4A3 produces six transcripts (T1-6), three longer (T3-5) than
315 others (T1,2,6) (Supplemental Fig. 6); the sequence of only the long transcripts overlaps with
316 ASTILCS. We designed LNAs targeting long isoforms of PTP4A3 (T3-5) – PTP-LONG-LNA and
317 LNAs targeting two (T1,2) out of three short isoforms of PTP4A3. We could not design an LNA
318 targeting only isoform T6 because it completely overlaps with the long isoforms. Interestingly, we
319 found that knockdown of only the short PTP4A3 isoforms led to a dose-dependent decrease in
320 HCC cell survival (Fig. 4D, E). We also analyzed whether knockdown of the long PTP4A3 isoforms
321 can affect the expression of the short isoforms. With this mechanism in mind, we measured the
322 expression of the short isoforms in HUH7 HCC cells treated with LNAs targeting long isoforms
323 and observed no difference in expression (Supplemental Fig. 7). Because ASTILCS overlaps only
324 with the long PTP4A3 isoforms and their knockdown does not affect the expression of their short,
325 survival modulating counterparts, we conclude that ASTILCS silencing does not lead to a
326 decrease in cell survival via downregulation of PTP4A3 transcripts.

327 Finally, we studied whether knockdown of SLC45A and PTK2 itself can decrease HCC
328 cell survival. PTK2 has been previously shown to affect HCC cell survival, with PTK2 silencing in
329 HepG2 and HUH6 HCC cells lines reducing cell growth and inducing apoptosis [86]. Meanwhile,
330 SLC45A4 has not been reported to affect cell survival. We treated HUH7 HCC cells with LNAs
331 targeting SLC45A or PTK2 and measured cell survival. We observed that only knockdown of

332 PTK2 was associated with a decrease in HCC cell survival (Fig. 4F, G). Based on our results we
 333 conclude that ASTILCS knockdown might decrease HUH7 cell survival and induce apoptosis via
 334 downregulation of PTK2.



335 **Figure 4. Knockdown of ASTILCS results in dose-dependent downregulation of**
 336 **neighboring genes.** **A.** Genomic locus of ASTILCS. Expression of ASTILCS neighboring genes
 337 in HUH7 cells upon LNA-mediated ($n \geq 8$) (**B**) or shRNA-mediated ($n \geq 5$) (**C**) knockdown of
 338 ASTILCS. Cell survival ($n \geq 8$) (**D**) and gene expression ($n \geq 5$) (**E**) upon LNA-mediated silencing of
 339 PTP4A3 isoforms. Cell survival ($n \geq 9$) (**F**) and gene expression ($n \geq 5$) (**G**) upon LNA-mediated
 340 silencing of ASTILCS neighboring genes PTK2 or SCL45A, $n \geq 9$. All values are mean \pm SD,
 341 **** $p < 0.0001$; *** $p < 0.001$; ** $p < 0.01$; * $p < 0.05$.

343
 344
 345

346 DISCUSSION

347 Despite recent progress in HCC management, it remains the second deadliest cancer type
348 with a 5-year relative patient survival rate of only 18% [1]–[4]. A better understanding of HCC
349 biology informs the development of more efficient treatment strategies. An increasing number of
350 studies suggests a vital role for lncRNAs in HCC progression [32], [87], [88]. However, their
351 functions in HCC biology remain largely unexplored. To address that problem, in our study, we
352 performed an shRNA-based pooled functional genetic screen to find lncRNAs that play crucial
353 roles in HCC cell progression. Applying stringent filtering criteria and three-step validation we
354 identified lncRNAs ASTILCS to be important for survival of HCC cells. To the best of our
355 knowledge, we provide the first characterization of the lncRNA ASTILCS. Following a framework
356 suggested by Joung et al in [43] we determined that ASTILCS is a nuclear lncRNAs with a local
357 regulatory mechanism. Using gene manipulation techniques, we demonstrated that ASTILCS
358 loss-of-function results in apoptosis and downregulation of the neighboring gene PTK2,
359 suggesting a possible mechanism of ASTILCS antisurvival effect.

360 PTK2, also known as Focal Adhesion Kinase, is a protein tyrosine kinase that plays an
361 essential role in formation of cell-matrix junctions (focal adhesion), regulation of cell migration,
362 and viability in a variety of cell types [89]–[92]. PTK2 recruitment to focal adhesions triggers PTK2
363 phosphorylation, creating a docking site for SH2 domain-containing proteins (Grb2, Shc etc), thus,
364 linking PTK2 to the activation of the pro-proliferative and anti-apoptotic RAS pathway. Besides
365 that, under certain cellular stress conditions, PTK can be recruited to the nucleus to facilitate
366 Mdm2-dependent ubiquitination of tumor suppressor protein p53 and downregulate apoptosis
367 [93]. Multiple studies report on the importance of PTK2 for cancer progression [94], [95]. To date
368 a few PTK2 inhibitors have been studied in clinical trials, however, the best observed response
369 was stable disease [96]–[98]. Understanding of mechanisms of PTK2 regulation might help to
370 develop more effective PTK2-targeting therapies. Recently, two independent scientific groups
371 simultaneously demonstrated that PTK2 is essential for HCC formation and growth *in vivo*
372 because of its role in activation of the WNT/b-catenin signaling. PTK2 overexpression stimulated
373 β -actin accumulation in the cell nucleus, thereby enhancing transcription of β -actin target genes
374 and promoting hepatocarcinogenesis. PTK2 silencing, on the other hand, led to increase in
375 apoptosis and a decrease in tumor growth [99], [100]. Thus, PTK2 downregulation by ASTILCS
376 knockdown can be an important factor mediating the mechanism of ASTILCS' proapoptotic effect
377 in HCC cells.

378 The molecular mechanisms of ASTILCS increasing PTK2 expression will require further
379 studies. Epigenetic regulation might be one of the possible mechanisms. PTK2 is overexpressed
380 in 30-60% of HCC patients and is associated with a higher metastasis rate and reduced survival.
381 Meanwhile, PTK2 expression in healthy liver tissues is negligible, which underlines the
382 importance of PTK2 expression for HCC progression [101]–[104]. In this study, we found that
383 ASTILCS levels were also significantly increased in HCC samples compared to normal tissues.
384 Interestingly, DNA sequence analysis in HCC patient samples revealed that PTK2 is amplified in
385 only 19-26% of cases and mutated in 2.5% [11], [99], [105]–[107]. Therefore, there should be
386 additional epigenetic mechanisms activating PTK2 expression. Examination of the PTK2
387 promoter demonstrated that the total methylation level of its CpG islands negatively correlated
388 with PTK2 gene expression. Thus, promoter demethylation might be a mechanism of PTK2
389 overexpression. Indeed, treatment of HCC cells with a demethylation agent has shown to increase
390 PTK2 mRNA and protein levels [99]. Some lncRNAs are known to affect DNA methylation via
391 direct interaction with DNA methyltransferases (DNMTs) or via indirect recruitment of DNMTs
392 through an intermediate protein [108]. Hence, the aforementioned evidence creates a possibility
393 that ASTILCS can increase PTK2 expression via regulation of its promoter methylation.

394 In addition to examination of ASTILCS effects on PTK2, we explored its relationship with
395 other neighboring genes. One of them, SLC45A4, is a proton-associated sucrose transporter, for
396 which there are no reports of direct association with cancer or cell survival (PubMed search on

397 03-24-2020). In this study, we demonstrate for the first time, that ASTILCS knockdown leads to
398 SLC45A4 silencing and that SLC45A4 silencing doesn't affect cell survival in HCC cells.
399 Surprisingly, we did not observe an obvious correlation between knockdown of antisense lncRNA
400 ASTILCS and expression of its sense protein-coding pair, PTP4A3 gene.

401 Thus, we inferred that the decrease in HCC cell survival upon ASTILCS knockdown is not
402 likely mediated by changes in PTP4A3 expression. PTP4A3, also known as Phosphatase of
403 Regenerating Liver 3 (PRL-3), is a protein-tyrosine phosphatase implicated in both cell
404 proliferation and invasion in several types of cancer, including HCC [109]–[112]. Despite the
405 importance of PTP4A3 for HCC cell survival, it seems the pro-survival effect of PTP4A3 is not
406 regulated by ASTILCS RNA expression. Yet, this does not exclude the existence of other
407 regulatory mechanisms between ASTILCS and PTP4A3 nor their importance in still undiscovered
408 cell functions. Interestingly, the functional analysis of PTP4A3 transcripts presented here
409 suggests that different transcripts affect cell survival in different ways in HCC cells. For the first
410 time, we report that only knockdown of short PTP4A3 transcripts (T1 and T2) reduces the cell
411 survival, while expression of the long transcripts (T3-T5) has no effect on cell viability. This finding
412 is in concordance with functional duality of PTP4A3, which is reported to regulate both cell survival
413 and metastasis. Given only the expression of short transcripts correlates with cell survival, we can
414 speculate that long transcripts might be involved in cell motility and invasion. This hypothesis
415 requires further exploration.

416 In summary, we identified and characterized a lncRNA, ASTILCS, which regulates HCC
417 cell survival presumably via activation of PTK2 expression and induction of apoptosis. In addition,
418 we unveiled the effects of ASTILCS neighboring genes, PTK2, SLC45A4 and PTP4A3, on HCC
419 cell survival. These findings provide valuable information about HCC biology and can advance
420 the development of future HCC treatments.

421

422 **ACKNOWLEDGMENTS**

423 This work was supported by the MIT Skoltech Initiative, Defense Advanced Research Projects
424 Agency (W32P4Q-13-1-001), S. Leslie Misrock Frontier Research Fund for Cancer
425 Nanotechnology, Translate Bio (Lexington, MA), and Koch Institute Support (core) Grant P30-
426 CA14051 from National Cancer Institute. We thank the Koch Institute Swanson Biotechnology
427 Center for technical support, specifically bioinformatics & computing, flow cytometry, genomics
428 (BioMicro Center) and high throughput screening. We also thank Prof. Philip Sharp (MIT) and
429 Prof. Timofei Zatsepin (Skoltech) for valuable discussions of the project, and Dr. Elena Smekalova
430 and Dr. Mikhail Nesterchuk (MIT) for technical support at different stages of the project.

431

432 **AUTHOR CONTRIBUTIONS**

433 Y.R. and R.B. designed the study; R.B. performed RNA sequencing and managed RNAi library
434 design; Y.R. executed the rest of the experiments, analyzed data and wrote the manuscript; J.G.
435 assisted with the experiments and edited the manuscript; Y.D. assisted with the experiments; V.C.
436 contributed to experimental design and execution, and edited the manuscript; C.V. analyzed next-
437 generation sequencing data; V.K. and D.A. supervised the study and edited the manuscript.

438

439 **DECLARATION OF INTERESTS:**

440 The authors declare no competing interests

441

442

443

444

445

446

447

448 **REFERENCES**

- 449 [1] S. Asia, S. Asia, and H. Hdi, "Liver Cancer Global WHO Report," vol. 876, pp. 2018–
450 2019, 2018, [Online]. Available: <http://gco.iarc.fr/today>.
- 451 [2] C. Allemani *et al.*, "Global surveillance of cancer survival 1995-2009: Analysis of
452 individual data for 25 676 887 patients from 279 population-based registries in 67
453 countries (CONCORD-2)," *Lancet*, vol. 385, no. 9972, pp. 977–1010, 2015, doi:
454 10.1016/S0140-6736(14)62038-9.
- 455 [3] C. Allemani *et al.*, "Global surveillance of trends in cancer survival 2000–14 (CONCORD-
456 3): analysis of individual records for 37 513 025 patients diagnosed with one of 18
457 cancers from 322 population-based registries in 71 countries," *Lancet*, vol. 391, no.
458 10125, pp. 1023–1075, 2018, doi: 10.1016/S0140-6736(17)33326-3.
- 459 [4] A. Villanueva, "Hepatocellular carcinoma," *N. Engl. J. Med.*, vol. 380, no. 15, pp. 1450–
460 1462, 2019, doi: 10.1056/NEJMra1713263.
- 461 [5] P. Rawla, T. Sunkara, P. Muralidharan, and J. P. Raj, "Update in global trends and
462 aetiology of hepatocellular carcinoma," *Współczesna Onkol.*, vol. 22, no. 3, pp. 141–150,
463 2018, doi: 10.5114/wo.2018.78941.
- 464 [6] American Cancer Society, "Cancer Facts and Figures 2020," Accessed: 28-Mar-2020.
465 [Online]. Available: <https://www.cancer.org/content/dam/cancer-org/research/cancer-facts-and-statistics/annual-cancer-facts-and-figures/2020/cancer-facts-and-figures-2020.pdf>.
- 466 [7] C. Allain, G. Angenard, B. Clément, and C. Coulouarn, "Integrative Genomic Analysis
467 Identifies the Core Transcriptional Hallmarks of Human Hepatocellular Carcinoma.,"
468 *Cancer Res.*, vol. 76, no. 21, pp. 6374–6381, Nov. 2016, doi: 10.1158/0008-5472.CAN-
469 16-1559.
- 470 [8] K. Okrah *et al.*, "Transcriptomic analysis of hepatocellular carcinoma reveals molecular
471 features of disease progression and tumor immune biology," *npj Precis. Oncol.*, vol. 2, no.
472 1, 2018, doi: 10.1038/s41698-018-0068-8.
- 473 [9] A. Ally *et al.*, "Comprehensive and Integrative Genomic Characterization of
474 Hepatocellular Carcinoma," *Cell*, vol. 169, no. 7, pp. 1327-1341.e23, 2017, doi:
475 10.1016/j.cell.2017.05.046.
- 476 [10] A. Fujimoto *et al.*, "Whole-genome sequencing of liver cancers identifies etiological
477 influences on mutation patterns and recurrent mutations in chromatin regulators," *Nat.*
478 *Genet.*, vol. 44, no. 7, pp. 760–764, 2012, doi: 10.1038/ng.2291.
- 479 [11] Z. Kan *et al.*, "Whole-genome sequencing identifies recurrent mutations in hepatocellular
480 carcinoma," *Genome Res.*, vol. 23, no. 9, pp. 1422–1433, 2013, doi:
481 10.1101/gr.154492.113.
- 482 [12] K. Schulze *et al.*, "Exome sequencing of hepatocellular carcinomas identifies new
483 mutational signatures and potential therapeutic targets," *Nat. Genet.*, vol. 47, no. 5, pp.
484 505–511, 2015, doi: 10.1038/ng.3252.
- 485 [13] H. Nakagawa, M. Fujita, and A. Fujimoto, "Genome sequencing analysis of liver cancer
486 for precision medicine," *Semin. Cancer Biol.*, vol. 55, no. November 2017, pp. 120–127,
487 2019, doi: 10.1016/j.semcancer.2018.03.004.
- 488 [14] K. Chaudhary, O. B. Poirion, L. Lu, S. Huang, T. Ching, and L. X. Garmire, "Multimodal
489 meta-analysis of 1,494 hepatocellular carcinoma samples reveals significant impact of
490 consensus driver genes on phenotypes," *Clin. Cancer Res.*, vol. 25, no. 2, pp. 463–472,
491 2019, doi: 10.1158/1078-0432.CCR-18-0088.
- 492 [15] J. J. Harding *et al.*, "Prospective genotyping of hepatocellular carcinoma: Clinical
493 implications of next-generation sequencing for matching patients to targeted and immune
494 therapies," *Clin. Cancer Res.*, vol. 25, no. 7, pp. 2116–2126, 2019, doi: 10.1158/1078-
495 0432.CCR-18-2293.
- 496 [16] Y. Hoshida *et al.*, "Integrative transcriptome analysis reveals common molecular
497
498

- 499 subclasses of human hepatocellular carcinoma,” *Cancer Res.*, vol. 69, no. 18, pp. 7385–
500 7392, 2009, doi: 10.1158/0008-5472.CAN-09-1089.
- 501 [17] K. Schulze, J. C. Nault, and A. Villanueva, “Genetic profiling of hepatocellular carcinoma
502 using next-generation sequencing,” *J. Hepatol.*, vol. 65, no. 5, pp. 1031–1042, 2016, doi:
503 10.1016/j.jhep.2016.05.035.
- 504 [18] G. Khemlina, S. Ikeda, and R. Kurzrock, “The biology of Hepatocellular carcinoma:
505 Implications for genomic and immune therapies,” *Mol. Cancer*, vol. 16, no. 1, pp. 1–10,
506 2017, doi: 10.1186/s12943-017-0712-x.
- 507 [19] “Identification and analysis of functional elements in 1% of the human genome by the
508 ENCODE pilot project,” *Nature*, vol. 447, no. 7146, pp. 799–816, Jun. 2007, doi:
509 10.1038/nature05874.
- 510 [20] “An integrated encyclopedia of DNA elements in the human genome,” *Nature*, vol. 489,
511 no. 7414, pp. 57–74, Sep. 2012, doi: 10.1038/nature11247.
- 512 [21] T. Derrien *et al.*, “The GENCODE v7 catalog of human long noncoding RNAs: Analysis of
513 their gene structure, evolution, and expression,” *Genome Res.*, vol. 22, no. 9, pp. 1775–
514 1789, Sep. 2012, doi: 10.1101/gr.132159.111.
- 515 [22] H. Jia, M. Osak, G. K. Bogu, L. W. Stanton, R. Johnson, and L. Lipovich, “Genome-wide
516 computational identification and manual annotation of human long noncoding RNA
517 genes,” *RNA*, vol. 16, no. 8, pp. 1478–1487, Aug. 2010, doi: 10.1261/rna.1951310.
- 518 [23] M. N. Cabili *et al.*, “Integrative annotation of human large intergenic noncoding RNAs
519 reveals global properties and specific subclasses.,” *Genes Dev.*, vol. 25, no. 18, pp.
520 1915–27, Sep. 2011, doi: 10.1101/gad.17446611.
- 521 [24] M. K. Iyer *et al.*, “The landscape of long noncoding RNAs in the human transcriptome,”
522 *Nat. Genet.*, vol. 47, no. 3, pp. 199–208, Mar. 2015, doi: 10.1038/ng.3192.
- 523 [25] M. Guttman *et al.*, “Chromatin signature reveals over a thousand highly conserved large
524 non-coding RNAs in mammals,” *Nature*, vol. 458, no. 7235, pp. 223–227, Mar. 2009, doi:
525 10.1038/nature07672.
- 526 [26] Y. Yang *et al.*, “Recurrently deregulated lncRNAs in hepatocellular carcinoma,” *Nat.*
527 *Commun.*, vol. 8, 2017, doi: 10.1038/ncomms14421.
- 528 [27] Q. Xia *et al.*, “Identification of novel biomarkers for hepatocellular carcinoma using
529 transcriptome analysis,” *J. Cell. Physiol.*, vol. 234, no. 4, pp. 4851–4863, 2019, doi:
530 10.1002/jcp.27283.
- 531 [28] H. Cui, Y. Zhang, Q. Zhang, W. Chen, H. Zhao, and J. Liang, “A comprehensive genome-
532 wide analysis of long noncoding RNA expression profile in hepatocellular carcinoma,”
533 *Cancer Med.*, vol. 6, no. 12, pp. 2932–2941, 2017, doi: 10.1002/cam4.1180.
- 534 [29] D. D. Esposti *et al.*, “Identification of novel long non-coding RNAs deregulated in
535 hepatocellular carcinoma using RNA-sequencing,” *Oncotarget*, vol. 7, no. 22, pp. 31862–
536 31877, 2016, doi: 10.18632/oncotarget.7364.
- 537 [30] C.-M. Wong, F. H.-C. Tsang, and I. O.-L. Ng, “Non-coding RNAs in hepatocellular
538 carcinoma: molecular functions and pathological implications.,” *Nat. Rev. Gastroenterol.*
539 *Hepatol.*, vol. 15, no. 3, pp. 137–151, Mar. 2018, doi: 10.1038/nrgastro.2017.169.
- 540 [31] X. Huo *et al.*, “Dysregulated long noncoding RNAs (lncRNAs) in hepatocellular
541 carcinoma: implications for tumorigenesis, disease progression, and liver cancer stem
542 cells.,” *Mol. Cancer*, vol. 16, no. 1, p. 165, Dec. 2017, doi: 10.1186/s12943-017-0734-4.
- 543 [32] M. Klingenberg, A. Matsuda, S. Diederichs, and T. Patel, “Non-coding RNA in
544 hepatocellular carcinoma: Mechanisms, biomarkers and therapeutic targets,” *J. Hepatol.*,
545 vol. 67, no. 3, pp. 603–618, Sep. 2017, doi: 10.1016/j.jhep.2017.04.009.
- 546 [33] P. McDonel and M. Guttman, “Approaches for Understanding the Mechanisms of Long
547 Noncoding RNA Regulation of Gene Expression.,” *Cold Spring Harb. Perspect. Biol.*, vol.
548 11, no. 12, p. a032151, Dec. 2019, doi: 10.1101/cshperspect.a032151.
- 549 [34] L.-L. Chen, “Linking Long Noncoding RNA Localization and Function,” *Trends Biochem.*

- 550 *Sci.*, vol. 41, no. 9, pp. 761–772, Sep. 2016, doi: 10.1016/j.tibs.2016.07.003.
- 551 [35] J. Carlevaro-Fita and R. Johnson, “Global Positioning System: Understanding Long
- 552 Noncoding RNAs through Subcellular Localization,” *Mol. Cell*, vol. 73, no. 5, pp. 869–883,
- 553 Mar. 2019, doi: 10.1016/j.molcel.2019.02.008.
- 554 [36] J. M. Engreitz *et al.*, “Local regulation of gene expression by lncRNA promoters,
- 555 transcription and splicing,” *Nature*, vol. 539, no. 7629, pp. 452–455, Nov. 2016, doi:
- 556 10.1038/nature20149.
- 557 [37] J. H. Noh, K. M. Kim, W. G. McClusky, K. Abdelmohsen, and M. Gorospe, “Cytoplasmic
- 558 functions of long noncoding RNAs,” *Wiley Interdiscip. Rev. RNA*, vol. 9, no. 3, p. e1471,
- 559 May 2018, doi: 10.1002/wrna.1471.
- 560 [38] D. E. Root, N. Hacohen, W. C. Hahn, E. S. Lander, and D. M. Sabatini, “Genome-scale
- 561 loss-of-function screening with a lentiviral RNAi library,” *Nat. Methods*, vol. 3, no. 9, pp.
- 562 715–719, Sep. 2006, doi: 10.1038/nmeth924.
- 563 [39] L. A. Gilbert *et al.*, “Genome-Scale CRISPR-Mediated Control of Gene Repression and
- 564 Activation,” *Cell*, vol. 159, no. 3, pp. 647–661, Oct. 2014, doi: 10.1016/j.cell.2014.09.029.
- 565 [40] M. Kampmann *et al.*, “Next-generation libraries for robust RNA interference-based
- 566 genome-wide screens,” *Proc. Natl. Acad. Sci.*, vol. 112, no. 26, pp. E3384–91, Jun. 2015,
- 567 doi: 10.1073/pnas.1508821112.
- 568 [41] J. Beermann *et al.*, “A large shRNA library approach identifies lncRNA Ntep as an
- 569 essential regulator of cell proliferation,” *Cell Death Differ.*, vol. 25, no. 2, pp. 307–318,
- 570 Feb. 2018, doi: 10.1038/cdd.2017.158.
- 571 [42] J.-F. Huang *et al.*, “Genome-wide screening identifies oncofetal lncRNA Ptn-dt promoting
- 572 the proliferation of hepatocellular carcinoma cells by regulating the Ptn receptor,”
- 573 *Oncogene*, vol. 38, no. 18, pp. 3428–3445, May 2019, doi: 10.1038/s41388-018-0643-z.
- 574 [43] J. Joung *et al.*, “Genome-scale activation screen identifies a lncRNA locus regulating a
- 575 gene neighbourhood,” *Nature*, vol. 548, no. 7667, pp. 343–346, Aug. 2017, doi:
- 576 10.1038/nature23451.
- 577 [44] I. Tiessen *et al.*, “A high-throughput screen identifies the long non-coding RNA DRAIC as
- 578 a regulator of autophagy,” *Oncogene*, vol. 38, no. 26, pp. 5127–5141, Jun. 2019, doi:
- 579 10.1038/s41388-019-0783-9.
- 580 [45] P. Cai *et al.*, “A genome-wide long noncoding RNA CRISPRi screen identifies *PRANCR*
- 581 as a novel regulator of epidermal homeostasis,” *Genome Res.*, vol. 30, no. 1, pp. 22–34,
- 582 Jan. 2020, doi: 10.1101/gr.251561.119.
- 583 [46] R. Galeev *et al.*, “Genome-wide RNAi Screen Identifies Cohesin Genes as Modifiers of
- 584 Renewal and Differentiation in Human HSCs,” *Cell Rep.*, vol. 14, no. 12, pp. 2988–3000,
- 585 Mar. 2016, doi: 10.1016/j.celrep.2016.02.082.
- 586 [47] S. E. Castel and R. A. Martienssen, “RNA interference in the nucleus: roles for small
- 587 RNAs in transcription, epigenetics and beyond,” *Nat. Rev. Genet.*, vol. 14, no. 2, pp. 100–
- 588 112, Feb. 2013, doi: 10.1038/nrg3355.
- 589 [48] R. Kalantari, C.-M. Chiang, and D. R. Corey, “Regulation of mammalian transcription and
- 590 splicing by Nuclear RNAi,” *Nucleic Acids Res.*, vol. 44, no. 2, pp. 524–537, Jan. 2016,
- 591 doi: 10.1093/nar/gkv1305.
- 592 [49] K. A. Lennox and M. A. Behlke, “Cellular localization of long non-coding RNAs affects
- 593 silencing by RNAi more than by antisense oligonucleotides,” *Nucleic Acids Res.*, vol. 44,
- 594 no. 2, pp. 863–877, Jan. 2016, doi: 10.1093/nar/gkv1206.
- 595 [50] S. Avivi *et al.*, “Visualizing nuclear RNAi activity in single living human cells,” *Proc. Natl.*
- 596 *Acad. Sci. U. S. A.*, vol. 114, no. 42, pp. E8837–E8846, 2017, doi:
- 597 10.1073/pnas.1707440114.
- 598 [51] L. S. Qi *et al.*, “Repurposing CRISPR as an RNA-Guided Platform for Sequence-Specific
- 599 Control of Gene Expression,” *Cell*, vol. 152, no. 5, pp. 1173–1183, Feb. 2013, doi:
- 600 10.1016/j.cell.2013.02.022.

- 601 [52] P. I. Thakore *et al.*, “Highly specific epigenome editing by CRISPR-Cas9 repressors for
602 silencing of distal regulatory elements,” *Nat. Methods*, vol. 12, no. 12, pp. 1143–1149,
603 Dec. 2015, doi: 10.1038/nmeth.3630.
- 604 [53] A. Goyal, K. Myacheva, M. Groß, M. Klingenberg, B. Duran Arqué, and S. Diederichs,
605 “Challenges of CRISPR/Cas9 applications for long non-coding RNA genes,” *Nucleic
606 Acids Res.*, p. gkw883, Sep. 2016, doi: 10.1093/nar/gkw883.
- 607 [54] X. Q. Lin, Z. M. Huang, X. Chen, F. Wu, and W. Wu, “XIST Induced by JPX Suppresses
608 Hepatocellular Carcinoma by Sponging miR-155-5p.,” *Yonsei Med. J.*, vol. 59, no. 7, pp.
609 816–826, Sep. 2018, doi: 10.3349/ymj.2018.59.7.816.
- 610 [55] Q. Kong *et al.*, “LncRNA XIST functions as a molecular sponge of miR-194-5p to regulate
611 MAPK1 expression in hepatocellular carcinoma cell,” *J. Cell. Biochem.*, vol. 119, no. 6,
612 pp. 4458–4468, Jun. 2018, doi: 10.1002/jcb.26540.
- 613 [56] S. Chang, B. Chen, X. Wang, K. Wu, and Y. Sun, “Long non-coding RNA XIST regulates
614 PTEN expression by sponging miR-181a and promotes hepatocellular carcinoma
615 progression.,” *BMC Cancer*, vol. 17, no. 1, p. 248, Dec. 2017, doi: 10.1186/s12885-017-
616 3216-6.
- 617 [57] W. Ma *et al.*, “Downregulation of long non-coding RNAs JPX and XIST is associated with
618 the prognosis of hepatocellular carcinoma.,” *Clin. Res. Hepatol. Gastroenterol.*, vol. 41,
619 no. 2, pp. 163–170, Mar. 2017, doi: 10.1016/j.clinre.2016.09.002.
- 620 [58] L. K. Zhuang *et al.*, “MicroRNA-92b promotes hepatocellular carcinoma progression by
621 targeting Smad7 and is mediated by long non-coding RNA XIST,” *Cell Death Dis.*, vol. 7,
622 no. 4, pp. e2203–e2203, Apr. 2016, doi: 10.1038/cddis.2016.100.
- 623 [59] J. Wan, D. Deng, X. Wang, X. Wang, S. Jiang, and R. Cui, “LINC00491 as a new
624 molecular marker can promote the proliferation, migration and invasion of colon
625 adenocarcinoma cells,” *Onco. Targets. Ther.*, vol. 12, pp. 6471–6480, 2019, doi:
626 10.2147/OTT.S201233.
- 627 [60] J. Li *et al.*, “Long non-coding RNAs expressed in pancreatic ductal adenocarcinoma and
628 lncRNA BC008363 an independent prognostic factor in PDAC,” *Pancreatology*, vol. 14,
629 no. 5, pp. 385–390, Sep. 2014, doi: 10.1016/J.PAN.2014.07.013.
- 630 [61] A. Sahakyan, Y. Yang, and K. Plath, “The Role of Xist in X-Chromosome Dosage
631 Compensation,” *Trends Cell Biol.*, vol. 28, no. 12, pp. 999–1013, Dec. 2018, doi:
632 10.1016/j.tcb.2018.05.005.
- 633 [62] D. Chen *et al.*, “Long noncoding RNA XIST expedites metastasis and modulates
634 epithelial–mesenchymal transition in colorectal cancer,” *Cell Death Dis.*, vol. 8, no. 8, pp.
635 e3011–e3011, Aug. 2017, doi: 10.1038/cddis.2017.421.
- 636 [63] C. Li *et al.*, “Long non-coding RNA XIST promotes TGF- β -induced epithelial-
637 mesenchymal transition by regulating miR-367/141-ZEB2 axis in non-small-cell lung
638 cancer,” *Cancer Lett.*, vol. 418, pp. 185–195, Apr. 2018, doi:
639 10.1016/j.canlet.2018.01.036.
- 640 [64] F. Xing *et al.*, “Loss of XIST in Breast Cancer Activates MSN-c-Met and Reprograms
641 Microglia via Exosomal miRNA to Promote Brain Metastasis,” *Cancer Res.*, vol. 78, no.
642 15, pp. 4316–4330, Aug. 2018, doi: 10.1158/0008-5472.CAN-18-1102.
- 643 [65] C. J. Echeverri and N. Perrimon, “High-throughput RNAi screening in cultured cells: a
644 user’s guide,” *Nat. Rev. Genet.*, vol. 7, no. 5, pp. 373–384, May 2006, doi:
645 10.1038/nrg1836.
- 646 [66] W. G. Kaelin and Jr, “Use and Abuse of RNAi to Study Mammalian Gene Function:
647 Molecular Biology,” *Science*, vol. 337, no. 6093, p. 421, 2012, doi:
648 10.1126/SCIENCE.1225787.
- 649 [67] P.-J. Volders *et al.*, “LNCipedia 5: towards a reference set of human long non-coding
650 RNAs,” *Nucleic Acids Res.*, vol. 47, no. D1, pp. D135–D139, Jan. 2019, doi:
651 10.1093/nar/gky1031.

- 652 [68] J. Li *et al.*, “TANRIC: An Interactive Open Platform to Explore the Function of lncRNAs in
653 Cancer,” *Cancer Res.*, vol. 75, no. 18, pp. 3728–3737, Sep. 2015, doi: 10.1158/0008-
654 5472.CAN-15-0273.
- 655 [69] T. S. Slordahl *et al.*, “The phosphatase of regenerating liver-3 (PRL-3) is important for IL-
656 6-mediated survival of myeloma cells.,” *Oncotarget*, vol. 7, no. 19, pp. 27295–27306, May
657 2016, doi: 10.18632/oncotarget.8422.
- 658 [70] Y.-X. Lian, R. Chen, Y.-H. Xu, C.-L. Peng, and H.-C. Hu, “Effect of protein-tyrosine
659 phosphatase 4A3 by small interfering RNA on the proliferation of lung cancer.,” *Gene*,
660 vol. 511, no. 2, pp. 169–176, Dec. 2012, doi: 10.1016/j.gene.2012.09.079.
- 661 [71] J. Zhang *et al.*, “miR-21, miR-17 and miR-19a induced by phosphatase of regenerating
662 liver-3 promote the proliferation and metastasis of colon cancer.,” *Br. J. Cancer*, vol. 107,
663 no. 2, pp. 352–359, Jul. 2012, doi: 10.1038/bjc.2012.251.
- 664 [72] Y. Matsukawa, S. Semba, H. Kato, Y.-I. Koma, K. Yanagihara, and H. Yokozaki,
665 “Constitutive suppression of PRL-3 inhibits invasion and proliferation of gastric cancer
666 cell in vitro and in vivo.,” *Pathobiology*, vol. 77, no. 3, pp. 155–162, 2010, doi:
667 10.1159/000292649.
- 668 [73] L. Wang *et al.*, “PTP4A3 is a target for inhibition of cell proliferatin, migration and invasion
669 through Akt/mTOR signaling pathway in glioblastoma under the regulation of miR-137.,”
670 *Brain Res.*, vol. 1646, pp. 441–450, Sep. 2016, doi: 10.1016/j.brainres.2016.06.026.
- 671 [74] J. Minshull and T. Hunt, “The use of single-stranded DNA and RNase H to promote
672 quantitative ‘hybrid arrest of translation’ of mRNA/DNA hybrids in reticulocyte lysate cell-
673 free translations,” *Nucleic Acids Res.*, vol. 14, no. 16, pp. 6433–6451, 1986, doi:
674 10.1093/nar/14.16.6433.
- 675 [75] H. Nakamura *et al.*, “How does RNase H recognize a DNA.RNA hybrid?,” *Proc. Natl.*
676 *Acad. Sci.*, vol. 88, no. 24, pp. 11535–11539, Dec. 1991, doi: 10.1073/pnas.88.24.11535.
- 677 [76] T. A. Vickers and S. T. Crooke, “The rates of the major steps in the molecular mechanism
678 of RNase H1-dependent antisense oligonucleotide induced degradation of RNA,” *Nucleic*
679 *Acids Res.*, vol. 43, no. 18, pp. 8955–8963, Oct. 2015, doi: 10.1093/nar/gkv920.
- 680 [77] G.-P. C. Mologni L, leCoutre P, Nielsen PE, “Additive antisense effects of different PNAs
681 on the in vitro translation of the PML/RARalpha gene,” *Nucleic Acids Res.*, vol. 26, no. 8,
682 pp. 1934–1938, Apr. 1998, doi: 10.1093/nar/26.8.1934.
- 683 [78] B. F. Baker *et al.*, “2'- O -(2-Methoxy)ethyl-modified Anti-intercellular Adhesion Molecule
684 1 (ICAM-1) Oligonucleotides Selectively Increase the ICAM-1 mRNA Level and Inhibit
685 Formation of the ICAM-1 Translation Initiation Complex in Human Umbilical Vein
686 Endothelial Cell,” *J. Biol. Chem.*, vol. 272, no. 18, pp. 11994–12000, May 1997, doi:
687 10.1074/jbc.272.18.11994.
- 688 [79] N. Dias and C. A. Stein, “Antisense Oligonucleotides: Basic Concepts and Mechanisms,”
689 *Mol. Cancer Ther.*, vol. 1, no. 5, pp. 347–355, Mar. 2002, Accessed: 03-May-2020.
690 [Online]. Available: <https://mct.aacrjournals.org/content/1/5/347.long>.
- 691 [80] C. F. Bennett and E. E. Swayze, “RNA Targeting Therapeutics: Molecular Mechanisms of
692 Antisense Oligonucleotides as a Therapeutic Platform,” *Annu. Rev. Pharmacol. Toxicol.*,
693 vol. 50, no. 1, pp. 259–293, Feb. 2010, doi: 10.1146/annurev.pharmtox.010909.105654.
- 694 [81] R. Kole, A. R. Krainer, and S. Altman, “RNA therapeutics: beyond RNA interference and
695 antisense oligonucleotides,” *Nat. Rev. Drug Discov.*, vol. 11, no. 2, pp. 125–140, Feb.
696 2012, doi: 10.1038/nrd3625.
- 697 [82] N. Gil and I. Ulitsky, “Regulation of gene expression by cis-acting long non-coding RNAs,”
698 *Nat. Rev. Genet.*, vol. 21, no. 2, pp. 102–117, Feb. 2020, doi: 10.1038/s41576-019-0184-
699 5.
- 700 [83] F. Kopp and J. T. Mendell, “Functional Classification and Experimental Dissection of
701 Long Noncoding RNAs,” *Cell*, vol. 172, no. 3, pp. 393–407, Jan. 2018, doi:
702 10.1016/j.cell.2018.01.011.

- 703 [84] O. Khorkova, A. J. Myers, J. Hsiao, and C. Wahlestedt, "Natural antisense transcripts,"
704 *Hum. Mol. Genet.*, vol. 23, no. R1, pp. R54–R63, Sep. 2014, doi: 10.1093/hmg/ddu207.
- 705 [85] V. Pelechano and L. M. Steinmetz, "Gene regulation by antisense transcription," *Nat.*
706 *Rev. Genet.*, vol. 14, no. 12, pp. 880–893, Dec. 2013, doi: 10.1038/nrg3594.
- 707 [86] D. Gnani *et al.*, "Focal adhesion kinase depletion reduces human hepatocellular
708 carcinoma growth by repressing enhancer of zeste homolog 2.," *Cell Death Differ.*, vol.
709 24, no. 5, pp. 889–902, May 2017, doi: 10.1038/cdd.2017.34.
- 710 [87] M. Lanzafame, G. Bianco, L. M. Terracciano, C. K. Y. Ng, and S. Piscuoglio, "The Role of
711 Long Non-Coding RNAs in Hepatocarcinogenesis.," *Int. J. Mol. Sci.*, vol. 19, no. 3, p. 682,
712 Feb. 2018, doi: 10.3390/ijms19030682.
- 713 [88] C. Li, J. Chen, K. Zhang, B. Feng, R. Wang, and L. Chen, "Progress and Prospects of
714 Long Noncoding RNAs (lncRNAs) in Hepatocellular Carcinoma.," *Cell. Physiol. Biochem.*,
715 vol. 36, no. 2, pp. 423–434, 2015, doi: 10.1159/000430109.
- 716 [89] J. T. Parsons, "Focal adhesion kinase: the first ten years," *J. Cell Sci.*, vol. 116, no. 8, pp.
717 1409–1416, Apr. 2003, doi: 10.1242/jcs.00373.
- 718 [90] S. K. Mitra, D. A. Hanson, and D. D. Schlaepfer, "Focal adhesion kinase: in command
719 and control of cell motility.," *Nat. Rev. Mol. Cell Biol.*, vol. 6, no. 1, pp. 56–68, Jan. 2005,
720 doi: 10.1038/nrm1549.
- 721 [91] M. D. Schaller, "Cellular functions of FAK kinases: insight into molecular mechanisms and
722 novel functions," *J. Cell Sci.*, vol. 123, no. 7, pp. 1007–1013, Apr. 2010, doi:
723 10.1242/jcs.045112.
- 724 [92] E. G. Kleinschmidt and D. D. Schlaepfer, "Focal adhesion kinase signaling in unexpected
725 places.," *Curr. Opin. Cell Biol.*, vol. 45, pp. 24–30, Apr. 2017, doi:
726 10.1016/j.ceb.2017.01.003.
- 727 [93] S.-T. Lim *et al.*, "Nuclear FAK Promotes Cell Proliferation and Survival through FERM-
728 Enhanced p53 Degradation," *Mol. Cell*, vol. 29, no. 1, pp. 9–22, Jan. 2008, doi:
729 10.1016/j.molcel.2007.11.031.
- 730 [94] F. J. Sulzmaier, C. Jean, and D. D. Schlaepfer, "FAK in cancer: mechanistic findings and
731 clinical applications," *Nat. Rev. Cancer*, vol. 14, no. 9, pp. 598–610, Sep. 2014, doi:
732 10.1038/nrc3792.
- 733 [95] N. Panera, A. Crudele, I. Romito, D. Gnani, and A. Alisi, "Focal Adhesion Kinase: Insight
734 into Molecular Roles and Functions in Hepatocellular Carcinoma.," *Int. J. Mol. Sci.*, vol.
735 18, no. 1, p. 99, Jan. 2017, doi: 10.3390/ijms18010099.
- 736 [96] T. Shimizu *et al.*, "A first-in-Asian phase 1 study to evaluate safety, pharmacokinetics and
737 clinical activity of VS-6063, a focal adhesion kinase (FAK) inhibitor in Japanese patients
738 with advanced solid tumors.," *Cancer Chemother. Pharmacol.*, vol. 77, no. 5, pp. 997–
739 1003, May 2016, doi: 10.1007/s00280-016-3010-1.
- 740 [97] N. F. Brown *et al.*, "A study of the focal adhesion kinase inhibitor GSK2256098 in patients
741 with recurrent glioblastoma with evaluation of tumor penetration of [11C]GSK2256098,"
742 *Neuro. Oncol.*, vol. 20, no. 12, pp. 1634–1642, Nov. 2018, doi: 10.1093/neuonc/noy078.
- 743 [98] S. F. Jones *et al.*, "A phase I study of VS-6063, a second-generation focal adhesion
744 kinase inhibitor, in patients with advanced solid tumors.," *Invest. New Drugs*, vol. 33, no.
745 5, pp. 1100–7, Oct. 2015, doi: 10.1007/s10637-015-0282-y.
- 746 [99] Z. Fan *et al.*, "PTK2 promotes cancer stem cell traits in hepatocellular carcinoma by
747 activating Wnt/ β -catenin signaling," *Cancer Lett.*, vol. 450, pp. 132–143, May 2019, doi:
748 10.1016/j.canlet.2019.02.040.
- 749 [100] N. Shang *et al.*, "Focal Adhesion Kinase and β -Catenin Cooperate to Induce
750 Hepatocellular Carcinoma," *Hepatology*, vol. 70, no. 5, pp. 1631–1645, Nov. 2019, doi:
751 10.1002/hep.30707.
- 752 [101] T. Fujii *et al.*, "Focal adhesion kinase is overexpressed in hepatocellular carcinoma and
753 can be served as an independent prognostic factor.," *J. Hepatol.*, vol. 41, no. 1, pp. 104–

- 754 11, Jul. 2004, doi: 10.1016/j.jhep.2004.03.029.
- 755 [102] S. Itoh *et al.*, “Role of expression of focal adhesion kinase in progression of
756 hepatocellular carcinoma.,” *Clin. Cancer Res.*, vol. 10, no. 8, pp. 2812–7, Apr. 2004, doi:
757 10.1158/1078-0432.ccr-1046-03.
- 758 [103] Z. Yuan, Q. Zheng, J. Fan, K. Ai, J. Chen, and X. Huang, “Expression and prognostic
759 significance of focal adhesion kinase in hepatocellular carcinoma,” *J. Cancer Res. Clin.*
760 *Oncol.*, vol. 136, no. 10, pp. 1489–1496, Oct. 2010, doi: 10.1007/s00432-010-0806-y.
- 761 [104] Y.-J. Jan *et al.*, “Overexpressed focal adhesion kinase predicts a higher incidence of
762 extrahepatic metastasis and worse survival in hepatocellular carcinoma.,” *Hum. Pathol.*,
763 vol. 40, no. 10, pp. 1384–90, Oct. 2009, doi: 10.1016/j.humpath.2009.03.006.
- 764 [105] H. Okamoto, K. Yasui, C. Zhao, S. Arii, and J. Inazawa, “PTK2 and EIF3S3 genes may
765 be amplification targets at 8q23-q24 and are associated with large hepatocellular
766 carcinomas.,” *Hepatology*, vol. 38, no. 5, pp. 1242–9, Nov. 2003, doi:
767 10.1053/jhep.2003.50457.
- 768 [106] K. Hashimoto *et al.*, “Analysis of DNA copy number aberrations in hepatitis C virus-
769 associated hepatocellular carcinomas by conventional CGH and array CGH,” *Mod.*
770 *Pathol.*, vol. 17, no. 6, pp. 617–622, Jun. 2004, doi: 10.1038/modpathol.3800107.
- 771 [107] J. Gao *et al.*, “Integrative analysis of complex cancer genomics and clinical profiles using
772 the cBioPortal.,” *Sci. Signal.*, vol. 6, no. 269, p. p11, Apr. 2013, doi:
773 10.1126/scisignal.2004088.
- 774 [108] Y. Zhao, H. Sun, and H. Wang, “Long noncoding RNAs in DNA methylation: new players
775 stepping into the old game.,” *Cell Biosci.*, vol. 6, no. 1, p. 45, Dec. 2016, doi:
776 10.1186/s13578-016-0109-3.
- 777 [109] J. Zhou, S. Wang, J. Lu, J. Li, and Y. Ding, “Over-expression of phosphatase of
778 regenerating liver-3 correlates with tumor progression and poor prognosis in
779 nasopharyngeal carcinoma.,” *Int. J. cancer*, vol. 124, no. 8, pp. 1879–86, Apr. 2009, doi:
780 10.1002/ijc.24096.
- 781 [110] W.-B. Zhao, Y. Li, X. Liu, L.-Y. Zhang, and X. Wang, “Evaluation of PRL-3 expression,
782 and its correlation with angiogenesis and invasion in hepatocellular carcinoma.,” *Int. J.*
783 *Mol. Med.*, vol. 22, no. 2, pp. 187–92, Aug. 2008, Accessed: 06-May-2020. [Online].
784 Available: <http://www.ncbi.nlm.nih.gov/pubmed/18636172>.
- 785 [111] C. Laurent *et al.*, “High PTP4A3 phosphatase expression correlates with metastatic risk in
786 uveal melanoma patients.,” *Cancer Res.*, vol. 71, no. 3, pp. 666–74, Feb. 2011, doi:
787 10.1158/0008-5472.CAN-10-0605.
- 788 [112] B.-H. Li, Y. Wang, C.-Y. Wang, M.-J. Zhao, T. Deng, and X.-Q. Ren, “Up-Regulation of
789 Phosphatase in Regenerating Liver-3 (PRL-3) Contributes to Malignant Progression of
790 Hepatocellular Carcinoma by Activating Phosphatase and Tensin Homolog Deleted on
791 Chromosome Ten (PTEN)/Phosphoinositide 3-Kinase (PI3K)/AKT Signaling Path,” *Med.*
792 *Sci. Monit.*, vol. 24, pp. 8105–8114, Nov. 2018, doi: 10.12659/MSM.913307.
- 793 [113] B. Langmead, C. Trapnell, M. Pop, and S. L. Salzberg, “Ultrafast and memory-efficient
794 alignment of short DNA sequences to the human genome.,” *Genome Biol.*, vol. 10, no. 3,
795 p. R25, 2009, doi: 10.1186/gb-2009-10-3-r25.
- 796 [114] L. B and D. CN, “RSEM: Accurate Transcript Quantification From RNA-Seq Data With or
797 Without a Reference Genome,” *BMC Bioinformatics*, vol. 12, p. 323, Aug. 2011, doi:
798 10.1186/1471-2105-12-323.
- 799 [115] J. Moffat *et al.*, “A Lentiviral RNAi Library for Human and Mouse Genes Applied to an
800 Arrayed Viral High-Content Screen,” *Cell*, vol. 124, no. 6, pp. 1283–1298, Mar. 2006, doi:
801 10.1016/j.cell.2006.01.040.
- 802 [116] M. Marcel, *Embnet.news: European Molecular Biology Network newsletter.*, vol. 17, no.
803 1. EMBnet, Administration Office, 1994.
- 804 [117] H. Li and R. Durbin, “Fast and accurate short read alignment with Burrows-Wheeler

805 transform.,” *Bioinformatics*, vol. 25, no. 14, pp. 1754–60, Jul. 2009, doi:
806 10.1093/bioinformatics/btp324.
807 [118] H. Li *et al.*, “The Sequence Alignment/Map format and SAMtools.,” *Bioinformatics*, vol.
808 25, no. 16, pp. 2078–9, Aug. 2009, doi: 10.1093/bioinformatics/btp352.
809 [119] M. I. Love, W. Huber, and S. Anders, “Moderated estimation of fold change and
810 dispersion for RNA-seq data with DESeq2.,” *Genome Biol.*, vol. 15, no. 12, p. 550, 2014,
811 doi: 10.1186/s13059-014-0550-8.
812 [120] D. Wiederschain *et al.*, “Single-vector inducible lentiviral RNAi system for oncology target
813 validation,” *Cell Cycle*, vol. 8, no. 3, pp. 498–504, Feb. 2009, doi: 10.4161/cc.8.3.7701.
814 [121] J. G. Doench *et al.*, “Optimized sgRNA design to maximize activity and minimize off-
815 target effects of CRISPR-Cas9,” *Nat. Biotechnol.*, vol. 34, no. 2, pp. 184–191, Feb. 2016,
816 doi: 10.1038/nbt.3437.
817 [122] K. R. Sanson *et al.*, “Optimized libraries for CRISPR-Cas9 genetic screens with multiple
818 modalities,” *Nat. Commun.*, vol. 9, no. 1, p. 5416, Dec. 2018, doi: 10.1038/s41467-018-
819 07901-8.
820 [123] F. A. Ran, P. D. Hsu, J. Wright, V. Agarwala, D. A. Scott, and F. Zhang, “Genome
821 engineering using the CRISPR-Cas9 system,” *Nat. Protoc.*, vol. 8, no. 11, pp. 2281–
822 2308, Nov. 2013, doi: 10.1038/nprot.2013.143.
823 [124] N. C. Stewart SA, Dykxhoorn DM, Palliser D, Mizuno H, Yu EY, An DS, Sabatini DM,
824 Chen IS, Hahn WC, Sharp PA, Weinberg RA, “Lentivirus-delivered stable gene silencing
825 by RNAi in primary cells,” *RNA*, vol. 9, no. 4, pp. 493–501, Apr. 2003, doi:
826 10.1261/rna.2192803.
827 [125] Y. Sancak *et al.*, “The Rag GTPases Bind Raptor and Mediate Amino Acid Signaling to
828 mTORC1,” *Science (80-.)*, vol. 320, no. 5882, pp. 1496–1501, Jun. 2008, doi:
829 10.1126/science.1157535.
830 [126] B. Wang, X. Seed, “A PCR primer bank for quantitative gene expression analysis,”
831 *Nucleic Acids Res.*, vol. 31, no. 24, pp. 154e – 154, Dec. 2003, doi: 10.1093/nar/gng154.
832 [127] A. Spandidos, X. Wang, H. Wang, and B. Seed, “PrimerBank: a resource of human and
833 mouse PCR primer pairs for gene expression detection and quantification,” *Nucleic Acids*
834 *Res.*, vol. 38, no. suppl_1, pp. D792–D799, Jan. 2010, doi: 10.1093/nar/gkp1005.
835
836
837
838
839
840
841
842
843
844
845
846
847
848
849
850
851
852
853
854
855

856 **MATERIALS AND METHODS**

857 Cell culture. Human hepatocellular carcinoma HUH7 cell line was a gift from Dr. Jay
858 Horton (UT Southwestern Medical Center). HUH7 and HEK293ft cell lines were grown in
859 Dulbecco's modified Eagle's medium with L-glutamine (DMEM, Gibco™) supplemented with 4.5
860 mg/ml glucose, 50 ug/ml gentamicin sulfate (Sigma), 25 mM HEPES (Gibco™) and 10% heat-
861 inactivated fetal bovine serum (FBS, Gibco™). All cells were cultured at 37°C, 5% CO₂. When the
862 cells reached a 70-80% monolayer, they were detached from the flask using 0.25% Trypsin-EDTA
863 solution and split 1:10. Concentrations for selection agents were determined using killing curve:
864 2.5 ug/ml puromycin (Sigma), 0.75 mg/ml G-480 (Sigma).

865 RNA sequencing and data analysis. Samples were prepared using strand-specific Ribo-
866 Zero kit and RNA sequencing was performed by MIT BioMicro Center
867 ([https://openwetware.org/wiki/BioMicroCenter:Software#BMC-BCC Pipeline](https://openwetware.org/wiki/BioMicroCenter:Software#BMC-BCC_Pipeline)). Reads were
868 aligned to transcripts derived from the hg19 assembly and the Ensembl version 68 non-coding
869 RNA annotation (non-coding genes) or the full Ensembl 68 annotation (protein-coding genes)
870 using Bowtie version 1.01 [113] and gene expression was summarized using RSEM version 1.2.3
871 [114].

872 Genome-wide screening. Based on HUH7 RNA sequencing results (Supplemental Fig.1,
873 Supplemental Table1), we designed a library of 7873 shRNA vectors allowing to do knockdown
874 of the identified 1618 lncRNAs based on RNAi. The library was developed, synthesized and
875 packed into lentivirus by the RNAi Consortium at the Broad Institute [115]. The shRNA sequences
876 were assembled into a pLKO.1 lentiviral backbone (Addgene plasmid #10878), containing a
877 puromycin resistance marker to allow for the antibiotic selection of transduced cells. CMV-VSV-
878 G (Addgene plasmid #8454) and psPAX2 (Addgene plasmid #12260) plasmids were used for
879 lentiviral packaging. The lentiviral library contained four to five shRNAs per target lncRNA and
880 was applied at a low multiplicity of infection (MOI) equal to 0.3. Two days after lentiviral library
881 exposure, infected cells were selected for four days on puromycin. To assess effects of shRNAs
882 on cell survival, the selected cells were cultured for four more weeks maintaining an shRNA
883 representation of 500 (i.e. each shRNA was expressed on average by 500 cells). The input pooled
884 shRNA plasmid library before virus production was also sequenced and used as a control.

885 Next generation sequencing. Samples for Illumina sequencing were prepared following
886 “One Step PCR Preparation of Samples for Illumina Sequencing” protocol from The RNAi
887 Consortium (<https://portals.broadinstitute.org/gpp/public/resources/protocols>). Briefly, gDNA was
888 isolated using the QIAamp DNA Blood Maxi Kit (Qiagen). Illumina adapter sequences with 5-letter
889 barcodes were used to PCR amplify the shRNA-expressing cassette. The samples were
890 multiplexed and sequenced by MIT BioMicroCenter using HiSeq2000 platform. The samples were
891 processed using the BMC/BCC 1.5.2 pipeline (updated on 08/12/2016). Adapter sequence
892 GGAAAGGACGAGGTACC was trimmed from reads using Cutadapt version 1.4.2 [116]. Trimmed
893 reads were then aligned target consisting of the 7873 sequence shRNA library with BWA version
894 0.7.10 [117]. Mapped reads were summarized and parsed using SAMtools version 1.3 [118] and
895 custom Perl scripts. The resulting count table was tested for differential representation using
896 DESeq2 version 1.10.1 [119] running under R version 3.2.3. Differential expression data was
897 visualized using Tibco Spotfire Analyst version 7.11.1.

898 Molecular cloning. shRNAs from the library (Supplemental Table 2) were annealed and
899 cloned into a pLKO.1_neo plasmid (a gift from Sheila Stewart; Addgene plasmid # 13425 ;
900 <http://n2t.net/addgene:13425> ; RRID:Addgene_13425) using a protocol from [120]. Two shRNAs
901 designed to target mCherry were used as controls. Briefly, oligos were resuspended in water to
902 a final concentration of 100 uM. 11.25 ul of each oligo (top and bottom) were mixed with 2.5 ul of
903 10X annealing buffer (1M NaCl, 100 mM Tris-HCl, pH=7.4) and annealed at 95°C using a water
904 bath. The pLKO.1_neo plasmid was digested using AgeI and EcoRI restriction enzymes and
905 purified on 1% agarose gel. Next, oligo mixture was diluted 1:400 in 0.5X annealing buffer and
906 ligated with the digested pLKO.1_neo plasmid using T4 DNA ligase (3 h at RT). 2 ul of the ligation

907 mixture was used to transform 10 ul of One Shot competent Stbl3 E. coli cells (Invitrogen)
908 according to manufacturers' instructions. Transformed bacteria were plated on LB-agar plates
909 with 100 ug/mL ampicillin and incubated overnight. Individual colonies were picked, inoculated in
910 3 ml of LB with ampicillin to start miniprep cultures and incubated for 24 h. Miniprep DNA was
911 isolated using QIAGEN Plasmid Mini Kit (Qiagen). shRNA sequences were confirmed by Sanger
912 sequencing (performed by Quintara Biosciences).

913 sgRNAs (Supplemental Table 3) were designed using the Broad Institute's GPP sgRNA
914 Designer [121], [122]. Two sgRNAs targeting mouse XIST and blasted against human genome
915 and transcriptome were used as controls. Then, the sgRNAs were assembled into a plasmid
916 expressing dead Cas9 (dCas9, Cas9 without endonuclease activity) fused with a transcription
917 inhibitor, The Krüppel associated box (KRAB) transcriptional repression domain, in a lentiviral
918 backbone containing a puromycin resistance sequence (pLV hU6-sgRNA hU6C-dCas9-KRAB-
919 T2a-Puro, a gift from Charles Gersbach, Addgene plasmid # 71236 ; <http://n2t.net/addgene:71236>
920 ; RRID:Addgene_71236, [52]) using Golden Gate assembly reaction as described in [123]. 2 ul of
921 the ligation mixture were used to transform 10 ul of NEB Stable Competent E. coli (NEB)
922 according to manufacturers' instructions. Transformed bacteria were plated on LB-agar plates
923 with 100 ug/mL ampicillin and incubated overnight. Individual colonies were picked, inoculated in
924 3 ml of LB with ampicillin to start miniprep cultures and incubated for 24 h. Miniprep DNA was
925 isolated using QIAGEN Plasmid Mini Kit (Qiagen). sgRNA sequences were confirmed by Sanger
926 sequencing (performed by Quintara Biosciences).

927 To create a plasmid expressing ASTILCS, it's full sequence was used to substitute GFP
928 in TRC209 lentiviral plasmid (PGK-Hygro-EF1a-GFP, gift from the Broad GPP, [43]). The cloning
929 and sequence validation were done by Genscript Biotech.

930 Lentivirus production and transduction. For transduction, plasmids were packaged into
931 lentivirus through transfection of the plasmids with a packaging plasmid (psPAX2 was a gift from
932 Didier Trono (Addgene plasmid # 12260 ; <http://n2t.net/addgene:12260> ; RRID:Addgene_12260))
933 and an envelope plasmid (CMV-VSV-G was a gift from Bob Weinberg (Addgene plasmid # 8454;
934 <http://n2t.net/addgene:8454> ; RRID:Addgene_8454), [124]) using TransIT-LT1 Transfection
935 Reagent (Mirus Bio). 300 000 HEK293ft cells were plated per well into a 6-well plate and
936 incubated overnight. 0.4 ug PAX2, 0.15 VSV-G and 3.3 ug plasmid of interest were added to 600
937 ul Opti-MEM and mixed with an equal volume of Opti-MEM containing 4 ul of TransIT-LT1. The
938 mixture was incubated at RT for 20 min and transferred to the well. The volume was brought to
939 600 ml per well with the culture media and incubated overnight. On the following day, the media
940 was changed. Media with lentiviral particles was collected after 48 hs and snap-frozen in liquid
941 nitrogen. All shRNA/sgRNA plasmids were produced in parallel.

942 Arrayed screening.

943 Equal numbers of HUH7 cells (5000) were plated in a 96-well plate and transduced with
944 5ul of shRNAs or 2 ul of sgRNAs packed into lentiviral particles, so that each well received only
945 one type of shRNA/sgRNA. A plasmid expressing Green Fluorescent Protein (GFP) (pLJM1-
946 EGFP was a gift from David Sabatini (Addgene plasmid # 19319; <http://n2t.net/addgene:19319> ;
947 RRID:Addgene_19319), [125]), but not caring antibiotic resistance marker was also packed into
948 lentiviral particles and used as a positive control for transduction and antibiotic selection. After an
949 overnight incubation the cell media was changed. Two days after the lentiviral transduction, a
950 selection reagent (G-480 or puromycin, respectively) was added to the culture media to select for
951 cells containing the shRNA/sgRNA expressing plasmids. Once the selection was completed (i.e.
952 all non-infected GFP treated cells were dead), cell survival was measured using Cell Titer assay.

953 Cell survival assay. HUH7 cell survival was analyzed using the CellTiter-Glo®
954 Luminescent Cell Viability Assay according to the manufacturer's protocol. Luminescence was
955 measured with the microplate reader Tecan Infinite® 200 PRO.

956 Cell proliferation assay. Cells were plated at low density in 96-well plates (2000 cells/well).
957 Cell number analysis using cell titer assay was performed at 1, 2, 3 and 5 days afterwards. For

958 growth curves analysis, doubling time was calculated from the exponential portion of the cell
959 growth curve using the following equation: $Td = 0.693t/\ln(Nt/N0)$, where t—time (in days), N0—
960 initial cell number, Nt—cell number on day t.

961 Gene expression analysis. For single tube reactions (Fig. 2G) RNA was isolated using
962 Omega Bio-tek's E.Z.N.A.® Total RNA Kit I isolation kit according to manufacturers' instructions.
963 Separation and purification of cytoplasmic and nuclear RNA (Fig. 2E) were done using
964 Cytoplasmic and Nuclear RNA Purification Kit (Norgen Biotek Corp.) also following
965 manufacturers' instructions. Reverse transcription reaction was performed using Applied
966 Biosystems™ High-Capacity RNA-to-cDNA™ Kit and 1 ug of RNA. RNA levels were assessed
967 by qPCR using Power SYBR™ Green PCR Master Mix (Applied Biosystems™). For high-
968 throughput experiments RNA isolation, reverse transcription reaction, and qPCR was performed
969 using Power SYBR™ Green Cells-to-CT™ Kit (Ambion) according to manufacturers' instructions.
970 TaqMan Fast Advanced Master Mix (Applied Biosystems™) was used with TaqMan primers
971 (Hs01060665_g1 for ACTB and Hs01377184_m1 for ASTILCS). β -actin mRNA was used as a
972 housekeeping control. The RNA levels were first normalized to the level of β -actin and then to an
973 average value of the control group. All SYBR Green primers are listed in Supplemental Table 7.

974 LNA transfection. LNAs targeting ASTILCS, SLC45A, PTK2 and PTP4A3 genes were
975 custom-designed using Qiagen's Antisense LNA GapmeR designer (Supplemental Table 4), and
976 non-targeting LNA (Negative Control A (NCA)) was included as a control. LNAs were
977 resuspended in water to a final concentration of 50 μ M. 10 000 HUH7 cells were plated per well
978 in a 96-well plate and incubated overnight. LNAs were formulated with Lipofectamine 2000
979 (Invitrogen) in Opti-MEM (Gibco™) according to the manufacturer. Each well was treated with 50
980 μ l Opti-MEM containing 20 pmol LNA formulated and 0.25 μ l Lipofectamine 2000. Cell survival
981 and gene expression were measured 24h after transfection.

982 Apoptosis analysis was performed using In Situ Cell Death Detection Kit, TMR red (Roche)
983 according to manufacturers' instructions. Briefly, cells were collected using 0.25% Trypsin-EDTA
984 solution, fixed with 4% paraformaldehyde in PBS at RT for 30 min and permeabilized with 0.1%
985 Triton X-100 in 0.1% sodium citrate for 2 min on ice. Next, TUNEL reaction mixture was added to
986 the cells and incubated at 37°C for 60 min. TMB-positive cells were detected and counted using
987 BD FACSCelesta Flow Cytometer, at least 10,000 cells were analyzed per sample.

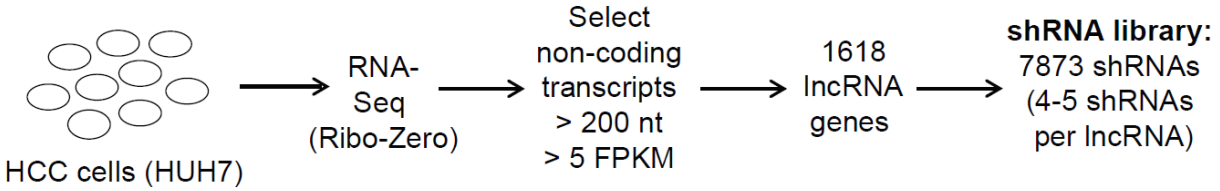
988 Statistical analysis. Statistical significance was calculated using GraphPad Prism 8.2
989 package. D'Agostino-Pearson omnibus normality test was used to establish whether or not the
990 population is distributed normally. Unpaired Mann-Whitney test was used to calculate the
991 difference between two different populations which are not normally distributed. One-way analysis
992 of variance (ANOVA) followed by Dunnett's post hoc test was used for multiple comparisons
993 analysis of normally distributed populations with equal variances (i.e. equal standard deviations
994 (SD)). Brown-Forsythe and Welch ANOVA tests followed by Dunnett's T3 multiple comparisons
995 analysis were used for normally distributed populations with different SDs. Kruskal-Wallis test
996 followed by followed by Dunn's multiple comparisons analysis was used for populations which are
997 not normally distributed.

998 Data Deposition. The sequence data has been submitted to the Gene Expression
999 Omnibus under superseries identifier GSE152651 which consists of the RNA-Seq data
1000 (GSE152650) and the shRNA screen data (GSE152649). Original data and numbers for tables
1001 are uploaded to Mendeley Data (DOI: 10.17632/dggchs5s8m.1).

1009 **SUPPLEMENTAL MATERIAL**

1010

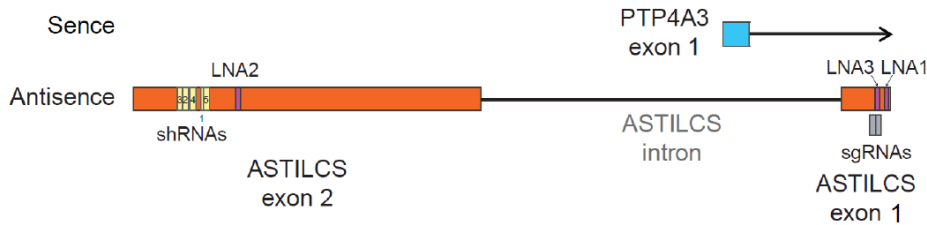
1011 **Supplemental Figure 1. Schematic workflow of shRNA library design.**



1012

1013

1014 **Supplemental Figure 2. Positions of shRNAs, sgRNAs and LNAs targeting ASTILCS.**

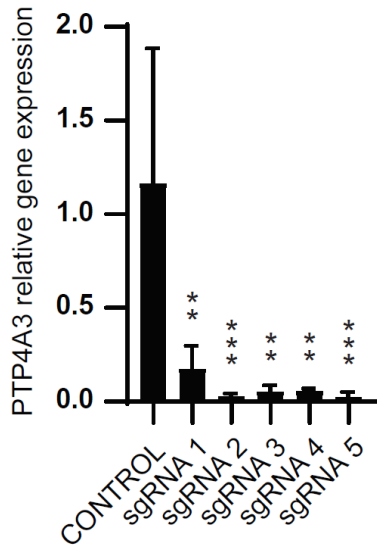


1015

1016

1017 **Supplemental Figure 3. PTP4A3 expression in HUH7 cells transduced with sgRNAs**

1018 **targeting ASTILCS TSS. n=12. All values are mean ± SD, **** p < 0.0001**



1019

1020

1021

1022

1023

1024

1025

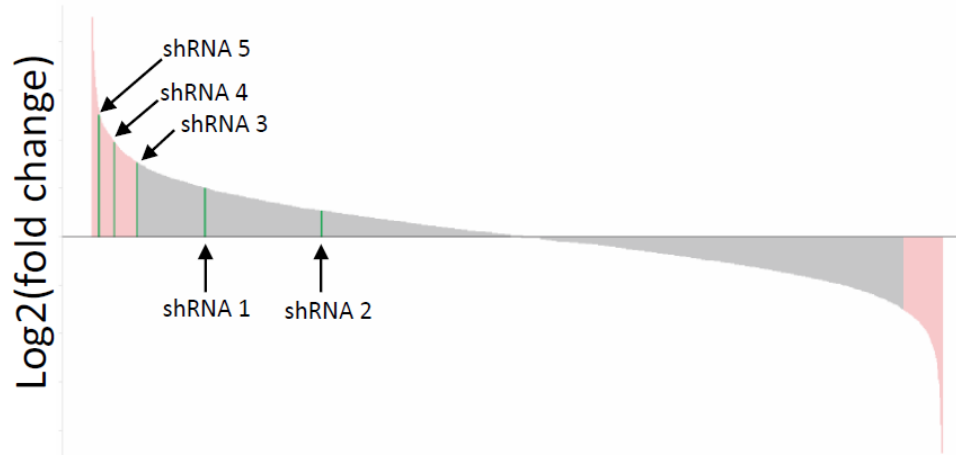
1026

1027

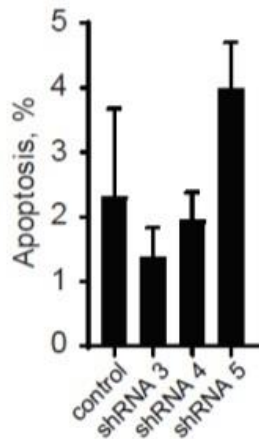
1028

1029

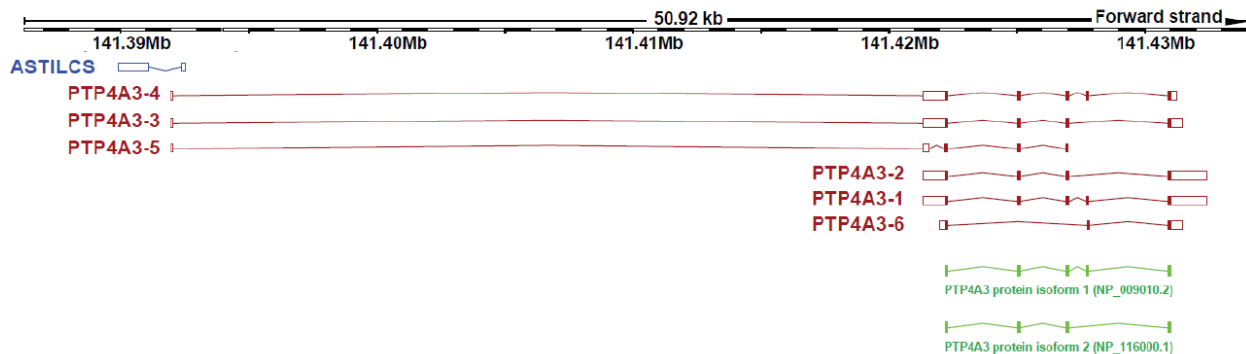
1030 **Supplemental Figure 4.** Waterfall plot of shRNAs present in the final population of HUH7 cells.
1031 $\text{Log}_2(\text{fold change}) > \text{ or } < 0.75$ is highlighted in light pink, shRNAs targeting ASTILCS are
1032 highlighted in green.



1033
1034
1035 **Supplemental Figure 5.** Apoptosis in HUH7 cells treated with shRNAs targeting ASTILCS, $n=3$.
1036 All values are mean \pm SD, there is no significant difference compared to control.
1037

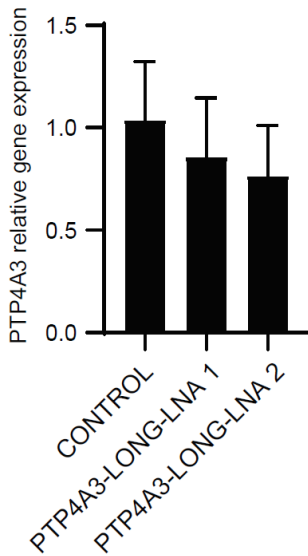


1038
1039
1040 **Supplemental Figure 6.** PTP4A3 gene produces 6 transcripts and 2 protein isoforms. Adapted
1041 from <http://www.ensembl.org/>.
1042



1043
1044

1045 **Supplemental Figure 7.** Expression of short PTP4A3 transcripts upon LNA-mediated
 1046 knockdown of long PTP4A3 transcripts, $n \geq 8$. All values are mean \pm SD, there is no significant
 1047 difference compared to control.



1048
 1049
 1050
 1051

Supplemental Table 1. Long non-coding RNA transcripts expressed in HUH7 cells. (Excel file)

Supplemental Table 2. shRNAs used for validation of the screen results

shRNA ID		Target sequence
Negative control	shRNA 1	ACTACGACGCTGAGGTCAAGA
	shRNA 2	GACTACTTGAAGCTGTCCTTC
ENST00000429829	shRNA 1	GCTCTTCTTTCACGCTTTATT
	shRNA 2	TCTTTGTGAACTGTGATTATT
	shRNA 3	TCATGTAATCTCTCCTTAAAT
	shRNA 4	TCTTAGACATATCTCTCATTT
	shRNA 5	ATCTCTTGCTGTTTGTGATTT
ASTILCS	shRNA 1	CACAGTGACTIONCACACTATAAT
	shRNA 2	AGACCAGCCTAGGTAACATA
	shRNA 3	GTGGGACCCTATCTCTACAAA
	shRNA 4	GGATCACTTGAGCCTAGGAAT
	shRNA 5	ACACTATAATCCCAGCAATTT
ENST00000518090	shRNA 1	TAACCAAATCACCTCACTGTC
	shRNA 2	CTTGCCCTTGGCCTCCAATAT
	shRNA 3	CTCAAATTCCTGGCCTCAAAC
	shRNA 4	ATGCTGGGATTACAGGCATG
	shRNA 5	CCTCACTGTCTCTCAAGAGAT
ENST00000510145	shRNA 1	CCTAGTGAGATGAACCCGGT
	shRNA 2	CTTTGACTCGGAAAGGGAECT
	shRNA 3	ACTTCCAGGTGCCGTCCATC
	shRNA 4	TGCAGAAATCACCAGTCTTCT
	shRNA 5	TTCCCGAGTGAGGCAATGCCT

ENST00000366097.2	shRNA 1	CCAAGTAGTTGGGATTATAGG
	shRNA 2	GAACTCCTGATCTCAGGTGAT
	shRNA 3	TTATAGGCGCTTGCCACCATG
	shRNA 4	GTTGGGATTATAGGCGCTTGC
ENST00000457084	shRNA 1	ATTGGGAAAGTTGACATTAAT
	shRNA 2	CTCATTATTCCTCACAGATTT
	shRNA 3	CTCATCTGAGCCTGGGCAAAT
	shRNA 4	ATCCAGGTCCTTCTCAGAGAA
	shRNA 5	TCGCGCAGAAGCTCCTCAATG
ENST00000421703.5	shRNA 1	GGAAC TTTATATTGCCATTTA
	shRNA 2	GGACCGATATTCTCCAGATTG
	shRNA 3	TGCTTGAGCCCAGGAGTTTGA
	shRNA 4	CAGCCTGGGCAACATGGCAA
	shRNA 5	GCCATTTAGAGGACCGATATT

1052

1053

Supplemental Table 3. sgRNAs used in the study

sgRNA ID	Target sequence
control sgRNA 1	TGTCAGAATTGCAATCTTTG
control sgRNA 2	TTGCAATTCTGACATCTTAT
ASTILCS:	
sgRNA 1	CGGGTCGTAGATGTCAGTGG
sgRNA 2	GGGCGGGTCGTAGATGTCAG
sgRNA 3	GGTCTGAGGCGGACTCCACC
sgRNA 4	CTGACATCTACGACCCGCCC
sgRNA 5	CACAGCCTTCCGTGCCTCCA
ENST00000518090:	
sgRNA 1	ACTGCCTACGAAAGCTGACC
sgRNA 2	ACAGTGAGGTGATTTGGTTA
sgRNA 3	TGAGAGACAGTGAGGTGATT
sgRNA 4	ATTTGGTTAAGGACAATTC
sgRNA 5	CAATTTCTGGTTCACATTCC
ENST00000366097.2:	
sgRNA 1	GGAAGTAGAAAGAAAGCACG
sgRNA 2	AGCACGAGGACCAGCCAGCT
sgRNA 3	GAGCAGGTGCTCCACAGACC
sgRNA 4	AAGCACGAGGACCAGCCAGC
sgRNA 5	GCTGGGAGAGGCCAGGTCTG
ENST00000421703.5:	
sgRNA 1	TATATCGATTCCTAACTTGG
sgRNA 2	AGATGGAAGGGAAGCCAACG
sgRNA 3	AACCACCCAGGGTTCCCCGT
sgRNA 4	TTAGATGGAAGGGAAGCCAA
sgRNA 5	CTATATCGATTCCTAACTTGG

1054 **Supplemental Table 4. LNAs used in the study**

ID	Qiagen cat. Number	Sequence
control LNA	LG00000002	AACACGTCTATACGC
ASTILCS - LNA 1	LG00193623	GGAAAGCAGAGCGTCA
ASTILCS - LNA 2	LG00193624	CGGCAATAGAAGCATT
ASTILCS - LNA 3	LG00193625	AGGGCGGGTCGTAGAT
SLC45A4-LNA 1	LG00230726	GAGGCGTCGTGGAAGA
SLC45A4-LNA 2	LG00230727	GCCGTTAAGGAAAAGT
PTK2-LNA 1	LG00230753	CCGAGTTAGCGGAATA
PTK2-LNA 2	LG00230754	TCGTCATAAGGCTGTA
PTP4A3-SHORT LNA 1	LG00230746	CCTTAGCCATCTGTCTG
PTP4A3-SHORT LNA 2	LG00230747	TGAGAAGCTGCCAAAT
PTP4A3-LONG LNA 1	LG00225103	CAGGATTTGGTTAAGC
PTP4A3-LONG LNA 2	LG00225104	ATGGATGCGCTCGGTA

1055
1056 **Supplemental Table 5. Population doubling time (Td) for HUH7 cells expressing GFP and**
1057 **ASTILCS. Td was calculated from the exponential portion of the cell growth curve (days 3-5) using**
1058 **the following equation: $Td = 0.693t/\ln(Nt/N0)$, where t—time (in days), N0—initial cell number,**
1059 **Nt—cell number on day t.**

	control	ASTILCS
replicate 1	1.17	1.16
replicate 2	1.07	1.13
replicate 3	1.02	1.10
replicate 4	1.02	1.11
average	1.07	1.13
Stand. Dev.	0.07	0.03
	p=0.1698	

1060
1061 **Supplemental Table 6. Expression (in FPKM) of genes in the ASTILCS locus in HUH7 cells.**

	AGO2	CHRAC1	DENND3	GPR20	MROH5	PTK2	SLC45A4	TRAPPC9	TSNARE1	ASTILCS
Replicate 1	9.98	28	1.99	0	0	49.04	13.27	3.99	0.49	22.26
Replicate 2	10.41	28.1	1.52	0	0	63.81	15.21	3.87	0.31	28.39
Replicate 3	8.89	23.14	1.92	0	0	58.63	11.54	3.24	0.32	23.27
Replicate 4	7.29	20.25	1.08	0	0	60.3	12.58	2.6	0.35	20.06

1062
1063 **Supplemental Table 7. SYBR Green primers used in the study.**

Gene ID	Forward primer sequence	Reverse primer sequence	PrimerBank ID [126], [127]
ACTB	CATGTACGTTGCTATCCAGGC	CTCCTTAATGTCACGCACGAT	4501885a1
AGO2	ACCCGCATCATCTTCTACCG	CTTGTCCCCCGCTCGTT	-
ASTILCS	TGCTTCTATTGCCGGGAAGTT	TAAAATGCAGCCACAGTGAAACG	-
CHRAC1	TCGTGGGTAAAGACAAGGGC	TGGCTAGGCATTGAACAAAGAG	342360617c1
DENND3	CCCATCCTGTCGGACCAGAT	GGACTTGGAGTAGGTGATGCT	50345869c3

ENST00000366097.2	TGGAGATCCAGCCATTACACA	AGTGTCCCTAAAGGGGAGGGG	-
ENST00000421703.5	TGGGGCAATTCCTATGGCTC	CTGTGACGGTTCCCAGAAGT	-
ENST00000518090	GCTGTGCACATCGAGAGAAG	AGGCCCATCGGGTGTATTG	-
PTK2	TGGTGCAATGGAGCGAGTATT	CAGTGAACCTCCTCTGACCG	313851041c2
PTP4A3	ACACATGCGCTTCCTCATCA	TCAATGAAGGTGCTGAGCGT	-
PTP4A3-LONG	CCTCCACCCGTCGTGC	CCCCTCCATGAACCCCAG	-
PTP4A3-SHORT	TGCCCTGTCCTGTCCTGATA	CACAGTCCCAAGAACCGTCA	-
SLC45A4	GCTGTCCCGTCCAAAGACC	GCAGACCCAATGAGAGGTGTG	122937258c1
TRAPPC9	TCCTCTACATCCGCTACAGGC	TGATGAGGCCACGACTTTG	238624121c1
TSNARE1	CCCCTAGAGTGCGCTAGATGT	GCCCTTGGGACAATAGGCG	254750703c1

1064